SRESA's International Journal of

LIFE CYCLE RELIABILITY AND SAFETY ENGINEERING

Vol.3 Issue No.3 July–Sept 2014 ISSN – 2250 0820

Special Issue :

On

"Selected Papers from NCRS-14"

Guest-Editors

Dr. M. Duraiselvam
Dr. P. Vaishnavi

Chief-Editors

P.V. Varde
A.K. Verma
Michael G. Pecht

SOCIETY FOR RELIABILITY AND SAFETY

Typeset & Printed

EBENEZER PRINTING HOUSE
Unit No. 5 & 11, 2nd Floor, Hind Services Industries,
Veer Savarkar Marg,
Dadar (west), Mumbai -28
Tel.: 2446 2632/ 3872
E-mail: outwork@gmail.com

Editorial

The SRESA National Conference on Reliability and Safety Engineering (NCRS-14) was organized jointly by Anna University, BIT Campus, Tiruchirappalli and Society for Reliability and Safety, Mumbai during 13 to 15 February 2014. The primary theme of the conference was reliability issues on critical systems, prognostics for electronic devices and safety assessment. In addition, some critical case studies were discussed in the conference which helped to bind research and development on real time applications in the areas of Reliability and Safety Engineering. Out of the nine papers selected for publication in the special issue on NCRS-14, six papers are included in the current issue and remaining papers will be published in the next issue. This special journal issue provides a glimpse into a few of high quality papers from various disciplines in the area of reliability and safety Engineering. All the selected papers are based on real-time application of technology range from Prognostics of electronic components, Reliability analysis on Passive systems, Reliability analysis of concrete bridges, Software Reliability Growth models for Safety systems, Manufacturing flaws for Electronic devices, Reliability of Programmable Logic Devices, Finite element simulation for Gas turbine applications, and Bayesian approach for software modeling.

The Guest editors would like to thank all the contributing authors for their outstanding research articles in the broad area within the stipulated time and effort devoted to the completion of their contributions. We hope that the research papers featured here sets a new milestone in the area of Reliability and Safety Engineering. We deeply acknowledge the support from Dr. Balaji Rao, Chief scientist, CSIR, for his in depth reviews and recommendations. In addition, we are thankful to Editors of SRESA Journal of Life Cycle Reliability and Safety Engineering for their kind invitation to edit this special issue.

Dr. M. Duraiselvam
Dr. P. Vaishnavi

	***Dr. M. Duraiselvam*** *is presently working as an Associate Professor in the Department of Production Engineering, National Institute of Technology, Tiruchirapalli. He completed B.E. in Mechanical Engineering from Coimbatore Institute of Technology in 1996 and M.E. in Manufacturing Technology from National Institute of Technology, Tiruchirapalli in 1998. He did his M.B.A. in Operations Management from Madurai Kamaraj University in 2002. He received his Ph.D. in Materials Science and Engineering from Technical University of Clausthal, Germany in 2006. His Research Interests are Laser Surface Engineering, Laser micromachining and Impact erosion studies. He received many awards and honors that include German Academic Exchange Service (DAAD) Fellowship from Germany, 3rd Best Paper for a presentation made in an International Conference held in Miami, Florida, USA and Young Scientist from DST. He is handling research projects worth more than 1 Crore from various funding sources such as DST, CSIR, BHEL, GTRE and DRDL. He has published 22-International Journals, 2-National Journals, 10-International and 4-National Conference presentations during his 14 years of tenure as a faculty. He is presently serving as a reviewer for many journals such as Surface & Coatings Technology, Surface and Interface Analysis, Materials Science and Engineering, Surface Engineering and Journal of Materials Processing Technology. He has delivered more than 30 invited talks and chaired sessions in conferences both at international and national level. He visited many countries like Germany, USA, France, Switzerland, Sweden, Singapore and Finland.*
	***Dr. P. Vaishnavi*** *is currently working as Assistant Professor in the Department of Computer Applications, Anna University, BIT Campus, Tiruchirappalli. She completed her doctoral programme in Reliability and Safety Engineering. She has more than 10 years of research and teaching experience in the areas of Reliability for Safety Critical Systems, Modeling of Dispersion studies of Radionuclides, Network Security, and Web services development in distributed computing. She has authored more than 30 articles including international journals, national conferences and proceedings. She has guided 20 post graduate students and taken short term courses for the students. Beyond the academic work, she is performing additional responsibility as Overall Coordinator, M.E degree programme in the mode of MBCBS for the professionals working in Affiliated/Polytechnic colleges of the University. At various levels in University she has organized Seminars, Conferences, Workshops and Exhibitions within the University and also collaborating with other Institutes/Organizations.*

Life Cycle Reliability and Safety Engineering
Vol.3 Issue 3 (2014) 01-07

Software Reliability Growth Model for Safety Systems of Nuclear Reactor

D. Thirugnana Murthy, T. Sridevi, K. Velusamy, N. Murali and S.A.V. Satya Murty
Indira Gandhi Centre for Atomic Research, Kalpakkam, Tamilnadu, India – 603102
dtm@igcar.gov.in

Abstract

The demand for complex software systems has increased more rapidly than the ability to design, implement, test, and maintain them, and the reliability of software systems has become a major concern for our modern society. Software failures have impaired several high visibility programs in space, telecommunications, defense and health industries. Besides the costs involved, it setbacks the project. The ways of quantifying and using it for improvement and control of the software development and maintenance process.

This paper discusses need for systematic approaches for measuring and assuring software reliability which is a major share of project development resources. It covers the reliability models with the concern on "Reliability Growth". It includes data collection on reliability, statistical estimation & prediction, metrics & attributes of product architecture, design, software development, and the operational environment. Besides its use for operational decisions like deployment, it includes guiding software architecture, development, testing and Verification & Validation.

Keywords: Software Reliability, Reliability Growth Model, metrics, Quality Assurance, Static Analysis

1. Introduction

Software design, development and testing have become very intricate with the advent of modern highly distributed systems, networks, middleware and interdependent applications. The demand for complex software systems has increased more rapidly than the ability to design, implement, test, and maintain them. So reliability of software systems has become a major concern. Today software is being deployed in safety applications due to the advancement of technology. In nuclear reactor many systems are being used in Safety critical and safety related applications, which demands high reliability [1, 2].

As software becomes an increasingly important part of many different types of systems that perform complex and critical functions in nuclear reactors, the risk and impacts of software caused failures have increased dramatically. There is now general agreement on the need to increase software reliability by eliminating errors made during software development [3].

This paper covers software reliability, the ways of quantifying it & using it for improvement and control of the software development and maintenance process. This paper also discusses need for systematic approaches for measuring and assuring *software reliability* which is a major share of project development resources. It covers the reliability models with the concern on "Reliability Growth". It includes data collection on reliability, statistical estimation & prediction, metrics & attributes of product architecture, design, software development, and the operational environment. Besides its use for operational decisions like deployment, it includes guiding software architecture, development, testing and Verification & Validation.

2. Software Reliability

Software reliability (SR) is defined as the probability of failure-free software operations in a specified environment. The software reliability field discusses ways of quantifying it and using it for improvement and control of the software development process. Software reliability is operationally measured by the number of field failures, or failures seen in development, along with a variety of ancillary information. The ancillary information includes the time at which the failure was found, in which part of the software it was found, the state of software at that time, the nature of the failure, *etc*[4].

Most quality improvement efforts are triggered by lack of software reliability. Thus, software managers recognize the need for systematic approaches to measure and assure *software reliability*, and devote a major share of project development resources to this. Almost one third of the total development budget is typically spent on testing, with the expectation of measuring and improving software reliability. A number of standards have emerged in the area of developing reliable software consistently and efficiently. ISO 9000-3 specifies measurement of field failures as the only required quality metric: "at a minimum, some metrics should be used which represent reported field failures and/or defects form the customer's viewpoint. The supplier of software products should collect and act on quantitative measures of the quality of these software products". The Software Engineering Institute has proposed an elaborate standard called the software Capability Maturity Model that scores software development organizations on multiple criteria and gives a numeric grade from one to five. A similar approach is taken by the SPICE standards, which is prevalent in Europe [5].

Formally, software reliability engineering is the field that quantifies the operational behavior of software-based systems with respect to user requirements with bearing on reliability. It includes data collection on reliability, statistical estimation, metrics and attributes of product architecture, design, software development, and the operational environment. Besides its use for operational decisions like deployment, it includes guiding software architecture, design, development, testing, *etc*. Indeed, much of the testing process is driven by software reliability concerns, and most applications of software reliability models are to improve the effectiveness of testing.

3. Need for Software Reliability Measurements & Ways to Quantify

Software is a collection of instructions or statements in a computer language. It is also called a computer program, or simply a program. A software program is designed to perform the specified functions. Upon execution of a program, an input state is translated into an output state. An input state can be defined as a combination of input variables or a typical transaction to the program. When the actual output deviates from the expected output, a failure occurs.

Within the last two decades many reported system outages or machine crashes were traced back to computer software failures. Radiation (Therac – 25) therapy software errors claimed several lives. In the telecommunications industry the network outages occurred in US-cities due to software problems in central office switches. Software failures have impaired in space, telecommunications, and defense and health industries. The Mars Climate Orbiter Mission Failure Investigation Board concluded 'The root cause, was the failed translation of English units into metric units in mission software' Current versions of the Osprey aircraft are not deployed because of software-induced field failures. The costly'Y2K"problem resulted because of a design failure.

3.1 Assessment

It is well recognized that assessing the reliability of software applications is a major issue in reliability engineering. Predicting software reliability is not easy. Perhaps the major difficulty is that it is concerned primarily with design faults, which is a very different situation from that tackled by conventional hardware theory. A *fault* (or bug) refers to a manifestation in the code of a mistake made by the programmer or designer with respect to the specification of the software. Activation of a fault by an input value leads to an incorrect output. Detection of such an event corresponds to an occurrence of a software *failure*. Input values may be considered as arriving to the software randomly. So although software failure may not be generated stochastically, it may be detected in such a manner. Therefore, it justifies the use of stochastic models of the underlying random process that governs the software failures.

3.2. Systematic approach

Verification and Validation (V & V) of the software systems are checking and analysis processes that ensure that software conforms to its specification and meets the needs of the customer. It encompasses testing. V &V is a whole life cycle process. The V & V procedure for Real Time Computers used for Safety Systems ensures the prevention of fault in Requirement, Design, Coding & maintenance. Software V&V processes "determine whether development products of a given activity conform to the requirements of that activity, and whether the software satisfies its intended use". It ensures Clarity, Correctness, Completeness, Consistency, and Compliance to standards and Traceability of each of the entity of the artifacts [6].

This determination includes analysis, evaluation, review, inspection, assessment, and testing of software products and processes are listed in Table 1[7]. The weightage for each stage of development process is marked in the scale of 10.The requirement stage is given more weights since removal of fault at this stage greatly reduces time, cost and improves reliability. In the same way testing & code becomes the important stages in enhancing reliability. V&V processes assess the software in the context of the system, including the operational environment, hardware, interfacing software, operators and users. By following the V & V process meticulously the software growth model can be used. In case of safety systems of Nuclear Reactor Internal V&V and External V&V becomes the mandatory. In view of this it is ascertained that the reliability increases in due course of time.

Table 1. Error Detection and Related Techniques

Technique	R (3)	D (1)	C (1)	T (2)	C (2)	M (1)
Algorithm analysis	✔	✔	✔	✔		✔
Boundary value analysis				✔		
Control flow analysis	✔	✔	✔			✔
Database analysis	✔	✔	✔	✔		✔
Data flow analysis	✔	✔	✔			✔
Data flow diagrams	✔					
Error seeding				✔		
Formal methods	✔	✔				
Code reading			✔			
Inspections	✔	✔	✔			
Interface analysis	✔	✔	✔			
Interface testing				✔		
Performance testing				✔		
Requirements parsing	✔					
Reviews	✔	✔	✔	✔	✔	✔
Simulation	✔	✔	✔	✔	✔	✔
Sizing & timing analysis		✔	✔	✔		✔
Stress testing				✔		
Traceability Analysis	✔	✔	✔	✔		
Prototyping	✔	✔	✔			
Regression analysis	✔	✔	✔	✔	✔	✔
Walkthroughs	✔	✔	✔	✔	✔	✔

R – Requirement, D- Design, C - Coding, T- Testing, CO – Code, M-Maintenance

3.3 Tools

Static analysis is basically analyzing the code without executing the software. Dynamic analysis consists of instrumenting code and executing test cases to measure the structural coverage achieved with the test cases.

An in-house developed "Static Analyzer of C program" is used to evaluate the quality attributes of the Code without executing. The following are the quailty attributes reported by the Static Analyzer [6]. Comment to Code Ratio, Cyclomatic Complexity, "Goto" statement,Ternary Operator, Nesting Level, Dynamic Memory, Unused Functions, Assembly Code and Unused & Un-initialsed variables[8].

Motor Industry Software Reliability Association (MISRA) "C" compliance ensures the "safe subset" of programming which guarantees the safety level. It has 127 rules with different severity levels, which makes the software simple, safe and maintainable. Other commercially available tools are also are used to produce Software Quality Assurance metrics and compared with each other.

4. Usage of Software Reliability

The SR is used to ascertain that the complete system is safe in conjunction with hardware. It ensures the safe, reliable operation of the nuclear plant. It also facilitates the order of comparison on Safety Critical and Safety related system. It can be demonstrated to the Inspectors, regulators and V&V teams with respect to engineered safety.

The software reliability demanded for the system as per the safety analysis of the complete nuclear planet forces the stakeholder in adhering to that value. Quantifying the SR in the beginning of the life cycle and iterating to the final stage validates the process methodology and acts as confidence building measure for the stakeholders.

5. Software Reliability Measuremnets & Reliability Models

Software reliability measurement includes two types of models called *static* and *dynamic* reliability estimation, used typically in the earlier and later stages of development respectively. One of the main weaknesses of many of the models is that they do not take into account ancillary information, like rapid changes in system during testing.

Two approaches are used in Software Reliability modeling. The most prevalent is the black-box

approach, in which only the interactions of the software with the environment are considered. Self-exciting point processes as a basic tool to model the failure process. This enables an overview of most of the SR models. A second approach, called the white-box approach, incorporates information on the structure of the software in the models, proposes basic techniques for calibrating black-box models. Fault prevention, fault removal and fault tolerance, which are three methods to achieve reliable software [9].

The reliability of software is a measure of the continuous delivery of the correct service by the software under a specified environment. This is a measure of the time to failure.

The first failure time is a random variable T with distribution function

$$F(t) = P\{T \leq t\} \quad t \varepsilon R$$

If F has a probability density function (p.d.f.) f, then the hazard rate of the random variable T by

$$r(t) = \frac{f(t)}{R(t)} \quad t \geq 0$$

with $R(t) = 1 - F(t) = P\{T > t\}$. Function R(t) is called the survivor function of the random variable T. The hazard rate function is interpreted to be

$$r(t)\,dt \approx P\{t < T \leq t + dt \mid T > t\}$$

$$\approx P\{\text{a failure occurs in } [t, t + dt] \text{ given that no failure occurred up to time } t\}$$

When F is continuous, the hazard rate function characterizes the probability distribution of T through the exponentiation

$$R(t) = \exp\left(-\int_0^t r(s)\,ds\right)$$

Finally, the mean time to failure is the expectation E[T] of the waiting time of the first failure. During the operational life of the software, repairs are carried out when it fails to perform correctly. In such a case, the time to repair, the time to reboot the system and other factors affect the dependability of a product. Thus, the software availability as a measure of the delivery correct service with respect to the alternation correct and incorrect service.

Failure process is assumed as a stochastic process. In other words, time is an essential component of the description of the models. On the other hand, static models are essentially capture-recapture models. Assumed that any corrective action is instantaneous and each detected fault is removed. A basic way to represent time evolution in confidence in software is as follows. At instant zero, the first failure occurs at time t_1 according a random variable $X_1 = T_1$ with hazard rate r_1. Given time $T_1 = t_1$, observe a second failure at time t_2 at rate r_2. Function r_2 is the hazard rate of the inter-failure random variable $X_2 = T_2 - T_1$ given $T_1 = t_1$. The choice of r_2 is based on the fact that one fault was detected at time t_1. At time t_2 a third failure occurs at t_3 with failure rate r_3. Function r_3 is the hazard rate of the random variable $X_3 = T_3 - T_2$ given $T_1 = t_1$, $T_2 = t_2$ and is selected according to the "past" of the failure process at time t_2, two observed failures at times t_1 and t_2 and so on. It is expected that, due to a fault removal activity, confidence in the software's ability to deliver a proper service will be improved during its life cycle. Therefore, a basic model in SR has to capture the phenomenon of reliability growth. Reliability growth will basically follow from a sequence of inequalities of the following form from selection of decreasing hazard rates r_i.

$$r_{i+1}(t - t_i) \leq r_i(t_i) \text{ on } t \geq t_i \quad \ldots\ldots\ldots\ldots \quad (1)$$

This "modeling process" is based on the Jelinski - Moranda model (JM). It is assumed that software includes only a finite number N of faults. The first hazard rate is $r_1(t; Ø, N) = ØN$, where Ø is some non-negative parameter. From time $T_1 = t_1$, a second failure occurs with the constant failure rate $r_2(t; Ø, N) = Ø(N-1)$. In a more formal setting, the two parameters N and Ø will be encompassed in what is called a background history f_0, which is any background information that may have about the software. An appealing graphical display of a path of this stochastic function is given in Figure 1. Stochastic intensity for the JM model is proportional to the residual number of bugs at any time t and each detection of failure results in a failure rate whose value decreases by an amount Ø. This suggests that no new fault is inserted during a corrective action and any bug contributes in the same manner to the "failure rate" of the software.

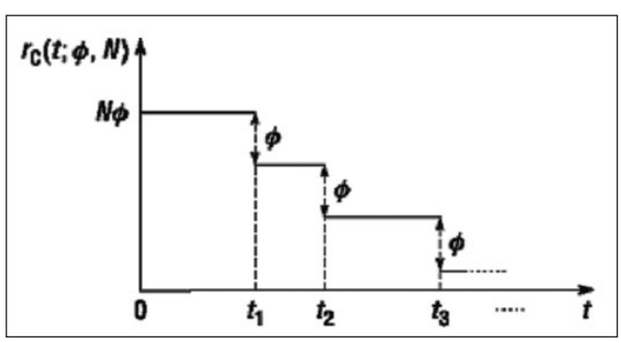

Figure1- Concatenated failure rate function for JM

It is understood that the stochastic intensity is excited by the history of the point process itself. Such a stochastic process is usually called a self-exciting point process (SEPP). The probability of at least two failures occurring in a time interval of length dt tends to zero at a rate higher than the probability that exactly one failure in the same interval does.

5.1 Static Models

One purpose of reliability models is to perform reliability prediction in an early stage of software development. This activity determines future software reliability based upon available software metrics and measures. Particularly when field failure data are not available (*e.g.* software is in the design or coding stage), the metrics obtained from the software development process and the characteristics of the resulting product can be used to estimate the reliability of the software upon testing or delivery. Two prediction models, the phase-based model by Gaffney and Davis and a predictive development life cycle model from Telcordia Technologies by Dalal and Ho exists.

5.2 Phase-based Model: Gaffney and Davis

Gaffney and Davis proposed the phase-based model, which divides the software development cycle into different phases (*e.g.* requirement, design, implementation, unit test, software integration, systems test, operation, *etc.*) and assumes that code size estimates are available during the early phases of development. Further, it assumes that faults found in different phases follow a Raleigh density function when normalized by the lines of code. Their model makes use of the fault statistics obtained during the early development phases (*e.g.* requirements review, design, implementation, and unit test) to predict the expected fault densities during a later phase(*e.g.* system test, acceptance test and operation). The key idea is to divide the stage of development along a continuous time and overlay the Raleigh density function with a scale parameter. The scale parameter, known as the *fault discovery phase constant*, is estimated by equating the area under the curve between earlier phases with observed error rates normalized by the lines of code. This method gives an estimate of the fault density for any later phase. This model also estimates the number of faults in a given phase by multiplying the fault density estimate by the number of lines of code.

5.3 Predictive Development Life Cycle Model

In Dalal & ho model the development life cycle is divided into the same phases. However, it does not postulate a fixed relationship (*i.e.* Raleigh distribution) between the numbers of faults discovered during different phases. Instead, it leverages past releases of similar products to determine the relationships. The relationships are not postulated beforehand, but are determined from data using only a few releases per product. Similarity is measured by using an empirical hierarchical Bayes framework.

The number of releases used as data is kept minimal, only the most recent one or two releases are used for prediction. This is critical, since there are often major modifications to the software development process over time, and these modifications change the inter-phase relationships between faults. The lack of data is made up by using as many products as possible that were being developed at the same time. In that sense it is similar to meta analysis, where a lack of longitudinal data is overcome by using cross-sectional data.

Conceptually, the basic assumptions behind this model are

Assumption 1: *Defect rates from different products in the same product life cycle phase are samples from a statistical universe of products coming from that development organization.*

Assumption 2: *Different releases from a given product are samples from a statistical universe of releases for that product.*

Assumption 1 reflects the fact that the products developed within the same organization at the same life cycle maturity are more or less homogeneous. The

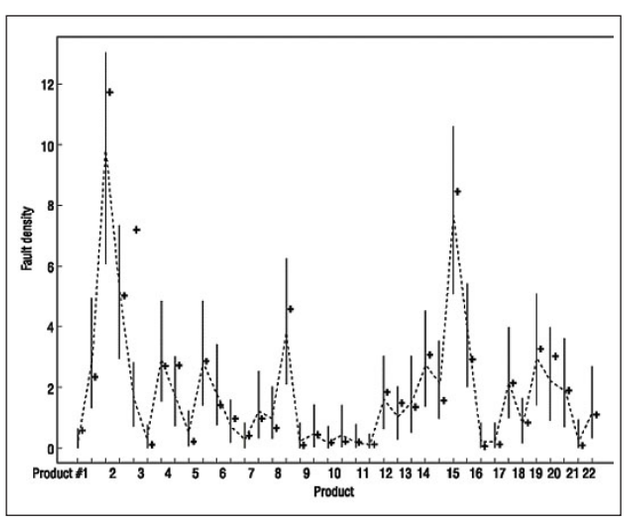

Figure :2 Products & their releases Vs observed (+) & predicted (dotted) fault density. Solid lines are 90% predictive intervals for fault density

homogeneity assumption is minimally restrictive, since the Bayesian estimates obtained which depend increasingly on the data, as more data become available. Based on the model described by Dalal and Ho, predictive distributions of the fault density per lifecycle phase conditionally on observing some of the previous product life cycle phases can be obtained. Figure 2 shows the power of prediction of this method. On the horizontal axis 22 products are there, each with either one or two releases. A dashed line connects the predicted fault density, and "+" indicates the observed fault density. Except for product number 4, all observed values are quite close to the predicted value.

5.4 Dynamic Models: Reliability Growth Models for Testing and Operational Use

Software reliability estimation determines the current software reliability by applying statistical inference techniques to failure data obtained during system test or system operation. Since reliability tends to improve over time because of removal of faults, the models are also called reliability growth models. The underlying failure process of the software, and use the observed failure history as a guideline, in order to estimate the residual number of faults in the software and the test time required to detect them.

5.5 A General Class of Models

In binomial models the total number of faults is *N*. It is found by time t has a binomial distribution with mean $\mu(t) = NF(t)$, where $F(t)$ is the probability of a particular fault being found by time t. Thus, the number of faults found in any interval of time (including the interval(t, ∞))is also binomial. $F(t)$ be any arbitrary cumulative distribution function. Then, a general class of reliability models is obtained by appropriate parameterization of $\mu(t)$ and N.

Letting N be Poisson (with some mean ν) gives the related Poisson model, the number of faults found in any interval is Poisson, and for disjoint intervals these numbers are independent. Denoting the derivative of F by F′, the hazard rate at time t is $F'(t) / [1 - F(t)]$. These models are Markovian, except when F is exponential, assumed the hazard rate to be an inverse linear function of time. For this "logarithmic Poisson" model is assumed which gives the total number of failures is infinite.

Let us examine the real example plotted in Figure 3 from testing a large software system at a telecommunications research company. The system

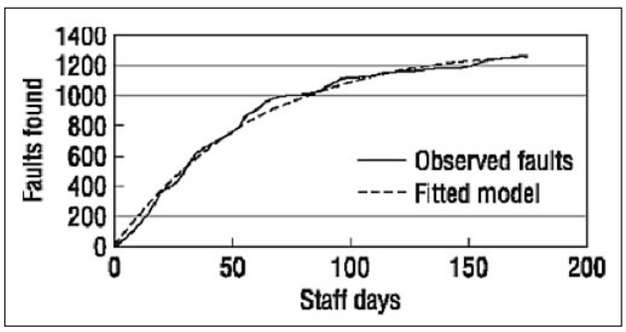

Figure: 3 The observed Vs fitted model

had been developed over years, and new releases were created and tested by the same development and testing groups respectively.

In Figure 3, the elapsed testing time in staff days t is plotted against the cumulative number of faults found for one of the releases where N being Poisson and F being exponential.

5.6. Precautions in Using Reliability Growth Models

In fitting any model to a given data set, first bearing is given model's assumptions. For example, a model assumes that a fixed number of software faults will be removed within a limited period of time. But in the observed process the number of faults is not fixed then use another model that does not make this assumption.

A second model limitation and implementation issue concerns future predictions. If the software is being operated in a manner different than the way it is tested (*e.g.* new capabilities are being exercised that were not tested before), the failure history of the past will not reflect these changes, and poor predictions may result. Development of operational profiles is very important when prediction of future reliability accurately in the user's environment.

Another issue relates to the software development environment. Most reliability growth models are primarily applicable from testing onward. The software is assumed to have matured to the point that extensive changes are not being made. These models cannot have a credible performance when the software is changing and churn of software code is observed during testing.

5.7 Assumptions in Reliability Growth Models

Different sets of assumptions can lead to equivalent models. Most of the models are based on underlying assumptions

1. The system being tested remains essentially unchanged throughout testing, except for the removal of faults.
2. Removing a fault does not affect the chance that a different fault will be found.
3. "Time" is measured in such a way that testing effort is constant.
4. The model is Markovian, *i.e.* at each time, the future evolution of the testing process depends only on the present state and not on the past history of the testing process.
5. All faults are of equal importance (contribute equally).
6. At the start of testing, there is some finite total number of faults, which may be fixed or random. Alternatively, the "number of faults" is not assumed finite.
7. Between failures, the hazard rate follows a known functional form, this is taken to be a constant.

6. Software Reliability Model for Safety Systems of Nuclear Reactor

Systematic approach is followed for design & development of safety system software of nuclear reactor. Internal and External V&V becomes the mandatory in the development process. In view of this it is ascertained that the reliability increases in due course of time, so the reliability growth model is assumed.

Software in safety systems of nuclear reactor is one-of-a- kind. So it is necessary to predict reliability at the requirement stage itself. Phase base model shall be used to predict the reliability for safety systems. In arriving the following parameters can be used.

- √ Number of Independent Specification Items (ISI)
- √ The complexity of each of the ISI, Levels 1,2,3
- √ Severity of V&V to be applied
- √ Kilo Lines of Deliverable Code by prediction methods
- √ Data on Fault Density & Removal of Similar Task
- √ Safety Classification of the system
- √ Tools validation including Compiler

Testing is very important phase in software development cycle. Testing is used to trigger, locate and remove software defects. As it progresses in the life cycle the reliability value is iterated with the actual value. This stage it calls for tuning and validating the development process. Various analysis tools such as trend analysis, fault - tree analysis, Orthogonal Defect classification and formal methods, etc, can also be used to minimize the possibility of defect occurrence after release and therefore improve software reliability.

7. Conclusion

There are many challenges in use of software reliability models. Part of the challenge is that testing and other activities are not as compartmentalized as assumed in models. Code churn constantly takes place during testing. Further, for decision-making purposes during testing and deployment phases it is preferable to have a quick estimate of the system reliability. Waiting to collect a substantial amount of data before being able to fit a model is not feasible in many situations. Leveraging information from the early phases of the development life cycle to come up with a quick reliable model would ameliorate this difficulty. It would also be worthwhile incorporating the architecture of the system to come up with preliminary estimates.

Acknowledgement

The authors gratefully acknowledge the constant support and motivation provided by Dr. Vasudeva Rao, Director IGCAR.

References

1. Design safety guide on computer based systems, Atomic Energy Regulatory Board / SG-D25.
2. Software reliability and safety in Nuclear reactor protection systems by J. Dennis Lawrence for U.S Nuclear regulatory commission. UCRL-ID-114839.
3. IEC 880 Software for computers in the Safety Systems of Nuclear Power Stations. IEC 1986.
4. Pressman, R.S., Software Engineering, McGraw Hill, 5th Ed., 2001.
5. Managing the software process. Watts S.Humphery, SEI series in software Engineering.
6. Sommerville, I., Software Engineering, Pearson Education, 6th Ed., 2001.
7. D. Thirugnana Murthy, T. Sridevi, A. Shanmugam, P. Swaminathan, Verification & Validation for Safety Critical Real Time Computers , International Journal on Intelligent Electronic Systems, Vol.1, No.1 Nov 2007, p.15-21.
8. T. Sridevi, A. Shanmugam, D.Thirugnana Murthy, S. Ilango Sambasivan, P. Swaminathan, Static Analyzer for Computer based Safety Systems, Journal Instrumentation Society of India. 37(1), pp.40-48, Mar 2007.
9. Reliability engineering handbook, Hoang Pham, Springer – Verlag londan limited, 2003.

Life Cycle Reliability and Safety Engineering
Vol.3 Issue 3 (2014) 08-12

Reliability Evaluation of Programmable Logic Devices

L. Srivani, D. Thirugnana Murthy, N. Murali and S.A.V. Satya Murty
Indira Gandhi Centre for Atomic Research, Kalpakkam, Tamilnadu, India – 603102
srivani@igcar.gov.in

Abstract

Programmable Logic Devices (PLD) are predominantly used as building modules in high integrity systems, considering their robust features such as high logic capacity, size, speed etc. PLDs are used to implement digital designs such as bus interface logic, control logic, sequencing logic, glue logic etc. Due to semiconductor evolution, new PLDs with state-of-the-art features are arriving to the market. Since these devices are reliable as per the manufacturer's specification, they were used in the design of safety systems. But due to their reduced market life, the availability of performance data is limited. So evaluating the PLD before deploying in a safety system is very important. This paper presents a survey on the use of PLDs in the nuclear domain and the steps involved in the evaluation of PLD using Quantitative Accelerated Life Testing.

Keywords: Accelerated tests, FPGA, PLD, QALT

1. Introduction

Programmable Logic Devices (PLD) are widely used as basic building modules in high integrity systems, considering their robust features such as gate density, performance, speed etc. In Instrumentation and Control (I&C) systems of Nuclear Power Plants (NPP), PLDs are used to implement digital designs such as bus interface logic, control logic, sequencing logic, glue logic etc. Since these devices are reliable as per the manufacturer's specification, they were used in the design of safety critical and safety related systems. But the availability of FPGA performance data in Nuclear Power Plants (NPP) is limited.

PLDs are highly reliable compared to using discreet logic devices, for their reduced circuit interconnections on the PCB (also easier troubleshooting). Nowadays pre-dispatch, device manufacturers employ Quality-Reliability engineering groups, who closely monitor each step of the design, manufacturing, packaging and burn-in process. This is performed to achieve more yield and high reliability. They mainly look for failure mechanisms. They even follow either traditional test methods or accelerated tests, to arrive at quantitative results on Mean Time To Failure (MTTF) values of the PLDs. Further to improve reliability, following practices are ensured. Device level, de-rating is followed in logic utilization, frequency of operation and power consumption. Board level, the devices are protected from electrical and thermal disturbances by subjecting the respective PCBs to signal integrity analysis and thermal analysis at design stage. Even the power supply to the PLDs is protected from transients by providing suppression circuits.

This paper covers a survey on the use of PLDs in the nuclear domain and the steps involved in the evaluation of PLD using Quantitative Accelerated Life Testing (QALT). The rest of this paper is organized as follows: an overview of PLDs and reliability tests are provided in section-2 and 3 respectively; section-4 presents a survey on the use of PLDs in the nuclear applications; the steps involved in performing the QALT are listed under section-5; finally the paper is concluded along with references and acknowledgements.

2. Programmable Logic Devices

Field Programmable Gate Array (FPGA) and Complex programmable Logic Devices (CPLD) are the popular PLDs among designers. A FPGA consists of an array of programmable logic modules (LM) and a programmable interconnecting area. The given design specification is captured using schematic mode or using hardware description language. Further it is converted to gate level netlist and configured on a FPGA by personalization followed by programming. Personalization is the process of selecting one of several possible configurations of a LM such that the LM performs as per the specification. A CPLD consists of programmable functional blocks named as *macrocell*, which contains logic implementing expressions and logic operations. The inputs and outputs of macrocells are connected together by global interconnection matrix, which is also reconfigurable. FPGAs are preferred for their high logic capacity whereas CPLDs are preferred for their predictable delays. A typical PLD design flow consists of steps such as design entry

(using schematic/ hardware description languages), functional simulation, synthesis, gate-level simulation, place & route, timing simulation and finally device programming. Later the silicon is tested on the prototype Printed Circuit Boards (PCB).

Programming is simply the process of implementing the chosen personalization within the given PLD. The final personalization of the PLD is done by the vendor's design tool without interaction or notification to the user. As the personalization is performed at the user's site, a test of the customized PLD can be only performed by the user after programming. However, before shipping the devices, the manufacturers test the device. This way programming failures can be eliminated or at least significantly decreased. In case of reprogrammable devices most of the possible personalization's are tested at the factory and the programming problems are reduced. The same is not applicable for one time programmable (OTP) devices. Usually OTP device manufacturers perform a function independent testing. The production testing of an OTP device utilizes a scan procedure.

Normally, the tests are performed at more than one accelerated stress level. The Reliability Engineer analyzes the test results for best fit in standard distributions (eg: exponential, weibull etc.) and arrives at overstress probability density function (*pdf*) for each accelerated stress level. Finally using life-stress relationship, the normal use level *pdf* is estimated based on the characteristics of overstress *pdf*'s. Arrhenius, Eyring, inverse power law, etc., are some of the life-stress relationship models available [1]. Among them, Arrhenius life-stress model is probably the most common life-stress relationship utilized in accelerated life testing, when the stress parameter is thermal (i.e. temperature). Further, failure analysis is performed in order to verify the reported failure and identify the mode or mechanism of failure as applicable. The root cause of the failure is ascertained by visual inspection of the device, electrical and functional failure, x-ray imaging, infra red imaging, C-mode scanning acoustic microscopy (CSAM), de-capsulation and scanning electron microscope.

3. Reliability Tests

Reliability tests are a set of tests performed on a product, indicate how it performs during its intended life. Essentially these tests are conducted to improve: quality by identifying design flaws and defects; reliability by lower field failures and finally to raise customer satisfaction. In view of long mission life's demanded by most of the applications today, it consumes more time to evaluate a product's long term behavior at normal operating conditions [1]. Earlier standards such as MIL-STD-781D [2], MIL-HDBK-781 [3] and IEC 60605 series [4] had guidelines for realistic combined stress, operational life/ mission profile reliability testing, but they are inactive today.

QALT[1] is designed to produce the data required for accelerated life data analysis. This analysis method uses life data obtained under accelerated conditions to extrapolate an estimated probability density function for the product under normal use conditions. Accelerated life tests are conducted on products to understand their failure modes and life characteristics. The products are subjected to enhanced stresses in order to force the products to fail early than they would normally, under use conditions. This process reduces test time.

Designing an accelerated test is a difficult task. Proper stress selection, application of stresses with control and maintenance of test unit's behavior and precipitating failure modes are very important steps to be followed. Especially the first time will be a learning experience. However as the targeted stress move farther away from the use conditions, the uncertainty in the extrapolation increases, for which confidence interval is considered [5].

QALT tests use either usage rate acceleration or overstress acceleration, to speed up the time-to-failure for the product under test. When the applied stress is more than the strength, the test unit fails. So higher stress levels help in reducing the test time. Applying more than one stress parameter accelerates certain failure mechanisms, which are caused by aging of the product. The need to extrapolate in both time and accelerating variables necessitates the use of fully parametric models [6]. William has listed several different failure mechanisms, their cause and the respective activation energy values [7].

Coming to the evaluation of FPGA technology, limited literature is available other than for space applications [8]. In 2004, IROC [9] conducted radiation tests on different technologies such as antifuse, flash, and SRAM. Though all three belong to CMOS, they observed antifuse technology was the most resistant to effects of radiation, while SRAM was the most susceptible. For space application, PLDs are selected and evaluated for possible design limitations and package related electric phenomena. One such is reported by Gustaffson & Hakansson in 2004 [10]. In

association with the vendor, they have tested a FPGA for electrical parameters such as ground bounce, VCC bounce, cross talk, rise time sensitivity and power consumption. An output pin switching from '1' to '0' or '0' to '1' is actually discharging or charging the capacitor that loads the I/O. When multiple output drivers switch at same time, they induce a voltage drop in the PLD power distribution. This momentarily raises the ground voltage within the device relative to the system ground. This apparent shift in the ground potential to a non-zero value is known as simultaneous switching noise or ground bounce. The same phenomenon is applicable to the VCC and is called VCC bounce. Cross talk is the result of capacitive and inductive coupling of a signal between signal lines. They indeed developed a stress design to find potential problems in FPGA.

4. PLD Applications in I&C of Nuclear Reactors

FPGA based implementations in safety critical I&C systems of NPP from the published literature is listed here. Few are developed for research purposes to evaluate suitability, build expertise and to replace the existing old technology and the rest are in development stages for upcoming NPPs.

1. **CANDU**: In 2009, She & Jiang [11] developed FPGA based logic for shutdown system number-1 for the CANadian Deuterium Uranium (CANDU) reactor. This was a feasibility study where they replaced the existing technology with FPGA. In 2010, Xing et al., [12] developed a FPGA based controller in CANDU reactor. Here the aim is to develop an FPGA development process that meets regulatory requirements and IEC standards for safety-critical system development.
2. **LUNGMEN:** An FPGA based *Reactor protection system* is reported by Lu et al., in 2010 [13], for the Lungmen NPP, which is still under construction.
3. **Wolf Creek:** At Wolf Creek generating station, the existing *Main Steam and Feedwater Isolation System* with old technologies is replaced with FPGAs. In 2009, USNRC granted the license [14].
4. **RPC Radiy:** The Ukrainian Research and Production Company (RPC) Radiy in association with Atomic Energy of Canada Ltd, introduced an FPGA development process, which meets regulatory requirements and IEC standards for safety critical system development [15-18]. The approach divided the FPGA component into two entities. Physically the FPGA has to be qualified as electronic hardware. The FPGA design using HDL code should follow a V-shape life cycle adapted from software by adding FPGA specific stages as described in IEC 62556 [19]. Using this platform, *Reactor trip system, Reactor power control and limitation system* etc, are implemented. Bakhmach et al., reported a FPGA based ESFAS (Engineered Safety Features of Actuation System) for Kozloduy NPP [15].
5. **IERICS mission:** An IAEA review mission titled "Independent Engineering Review of I&C Systems (IERICS) in NPP" was established in 2009. It has reviewed the FPGA based systems produced by RPC Radiy in 2010 [20].
6. **Electricite de France:** Rolls-Royce and Electricite de France has carried out modernization of 900MWe units. The Rod control system and Reactor in-core measurement system is replaced with FPGA technology [21].

The survey shows a growing interest in the use of FPGAs for safety critical I&C systems of NPP. The same is reflected through dedicated seminars/ conferences and guidelines (IEC62566, NUREG/CR-7006 [22], EPRI-2009 & 2011 [23, 24]). It is also observed that Actel's antifuse based and flash based FPGAs are used in the above implementations. There is one survey report on FPGA technology by Finnish research for NPP safety, covers the FPGA technology in Nuclear domain till 2012 [25].

5. **Accelerated Life Test and Data Analysis**

Normally the accelerated tests are failure terminated. i.e. the test is terminated on reaching the predefined number of failures. If no failures are observed, the environmental stress factors are raised in step fashion. Since the testing procedure involves time and cost, failures (if any) other than the device under test should be avoided to the maximum extent. The ALT for the devices is performed by placing them inside a test chamber. In Accelerated Life data analysis, the challenge is to determine the use level *pdf* from accelerated life test data. The objective of an ALT is to obtain the use level stress *pdf* by extrapolating the over stress *pdf*. First the stress parameters have to be identified. It can be single stress parameter or multiple stress parameters. Minimum two high stress levels data is required to map to a use stress level.

The steps involved are:

1. Plan for the Accelerated Life Test (ALT) – First create a testable design for the device under test (i.e PLD) and the associated PCB design. The entire design should be highly testable to find out whether the device has failed or not. A

testable circuit is one, in which a fault in any of the internal components onto which it is mapped can be detected by applying test vectors at its input pins and observing the values at its output pins over a period of time. Minimum neighboring circuitry recommended for generating test inputs and for checking the expected outputs. Because, adding additional devices for these functions pose problems during diagnosis of a failure as it will be difficult to determine the cause of failure (whether it was due to failure of the PLD or the failure of the supporting circuitry). Therefore the entire test setup has to be designed considering the test conditions and the associated chamber conditions.

2. Conduct experiment at various stress levels and collect of data for further analysis. For each stress level fresh sample is recommended. For the tests, the size of the test sample is governed by many factors including the test duration, cost, type of stresses applied, number of samples available and physical size.
3. Choose an appropriate life distribution – exponential, Weibull etc.
4. Select a Life-Stress relationship - Select a model that describes a "characteristic point" or a "life characteristic" of the distribution from one stress level to another. They include Arrhenius model, Eyring model etc. Table-1 lists the life characteristics of few distributions. Life characteristic is stress dependant.

Table 1: Life Characteristics

Distribution	Parameters	Life characteristics
Weibull	B, η	Scale parameter, η
Exponential	Λ	Mean Life (1/λ)
Lognormal	Ŧ, σ	Median, Ť
Normal	μ, σ	Mean, μ

5. Select a method to perform parameter estimation - For parameter estimation, either graphical method or Maximum Likelihood Estimation (MLE) method is used. The graphical method involves generating two types of plots. First, the life data at each individual stress level are plotted on a probability paper respective to the life distribution. This is performed using either Probability Plotting or Least Squares method. The parameters of the distribution at each stress level are then estimated from the plot. The second plot is drawn on a paper that linearizes the selected life-stress relationship based on the chosen life characteristic (scale parameter, mean life, etc). For this a special plotting paper is used which linearizes the life-stress relationship eg., a log-log paper. Further parameters are estimated by solving the slope and intercept of the line. Proper care has to be taken during manual probability plotting. The Least squares method requires that a straight line be fitted to a set of points such that the sum of the squares of the vertical derivations from the points to the line is minimized. Plotting methods cannot be employed for the tests terminated without failures. MLE treats both the life distribution and the life-stress relationship as one model and derives the shape parameter. Here the uncertainities are accounted in the form of confidence bounds. Though this method is simple, it is mathematically intense. For the same, dedicated tools are also available.
6. Once the *pdf* arrived, all other reliability information can be derived from it - For products with predominant temperature dependant failure mechanisms, the Arrhenius model is used. Arrhenius life-stress model is probably the most common life-stress relationship utilized in accelerated life testing, when the stress parameter is thermal (i.e. temperature). It is an exponential relationship with the basic assumption "life is proportional to the inverse reaction rate of the process", which is given by Eq(1)

$$L(V) = C.\ e^{(B/V)} \quad \text{------ Eq (1)}$$

Where,

L – Mean life

V – Stress level temperature in Kelvin

C – Model parameter to be determined, (C>0)

B – (Activation energy / Boltzman's constant)

Acceleration factor is the ratio of life between the use level stress and accelerated stress level as in Eq(2).

$$AF = L\_use/L\_Accelerated \quad \text{------ (2)}$$

7. Failure analysis of the failed PLD: In order to verify the reported failure, failure analysis has to be performed. First the physical damages have to be recorded. Second the electrical/ functional failure of the device has to be ascertained using curve tracing method on the I/O pins for continuity. The physical integrity of the PLD internals are checked using the x-ray imaging. CSAM is a non-destructive analysis technique, operates via a pulse/ echo technique, provides a method of unlayering the individual internal interfaces within the microelectronic package. Further CSAM and de-capsulation has to be performed based on the necessity. CSAM's use is for the detection of

delaminations between internal package interfaces and cracking of or void formations within die attach material. Especially used for moisture sensitivity [26]. De-capsulation, or de-cap, is a failure analysis technique which involves the removal of material packaging from an IC. It reveals any die level defect such as die crack, electrical over stress and die damage. It is performed either by Chemical etching or Mechanical etching. If required the die can be examined using the scanning electron microscope.

6. Conclusion

Designers are comfortable with PLDs for their robust features and also as economic replacement for application specific ICs. However, the use of PLDs in critical applications may raise concerns on their dependability. Though the devices are highly reliable as per the manufacturer's specification, performing reliability tests will raise the confidence level. For this QALT tests are one of the ideal way to evaluate the life of PLDs. Further it has to be extended to physics of failure approach.

Acknowledgement

The authors take this opportunity to acknowledge the constant support and motivation provided by Dr. P. R. Vasudeva Rao, Director IGCAR.

References

1. Accelerated Life testing, http://www.weibull.com/
2. MIL-STD-781D, "Reliability testing for engineering development, qualification and production
3. MIL-HDBK-781A, Reliability test methods, plans and environments for engineering development, qualification and production
4. IEC60605 series, "Equipment reliability testing" [5]. Managing the software process. Watts S.Humphery, SEI series in software Engineering.
5. Pantelis Vassiliou, Adamantios Mettas and Tarik El-Azzouzi, "Quantitative Accelerated Life-testing and Data Analysis", Handbook of Performability Engineering, Pages 543-557, 2008
6. Luis A. Escobar and William Q. Meeker, "A review of Accelerated test Models", Statistical science, Vol. 21, Institute of Mathematical statistics, 2006
7. William J. Vigrass, "Calculation of Semiconductor failure rates".
8. KLABS: http://klabs.org/richcontent/fpga_content/pages/notes/fpga_reliability.htm, "FPGA Reliability"
9. iRoC Technologies 2004. Radiation Results of the SER Test of Actel, Xilinx and Altera FPGA instances. 2004. Available at: http://www.actel.com/documents/RadResultsIROCreport.pdf
10. Per Gustafsson, "Evaluation of an FPGA for space applications", Department of Science and Technology, Master Thesis, Linkopings University, 2005
11. She J, Jiang J, "Application of FPGA to shutdown system No. 1 in CANDU", In: NPIC&HMIT 2009, 5–9 April, Knoxville, Tennessee.
12. Xing A, de Grosbois J, Archer P, Awwal A, Sklyar V, "FPGA-Based Controller in CANDU® Nuclear Safety-Reactor Applications", In: NPIC&HMIT 2010, 7–11 November, Las Vegas, Nevada, pp. 1337–1344
13. Lu, J.-J., Chou, H.-P., Wong, K.-W, "Conceptual design of FPGA-based RPS for the Lungmen Nuclear Power Plant", In: NPIC&HMIT 2010, 7–11 November, Las Vegas, Nevada, pp. 944–953
14. Dittman, B.F, "Licensing field-programmable gate arrays in safety systems",In: NPIC&HMIT 2010, 7–11 November, Las Vegas, Nevada, pp. 966–976.
15. Bakhmach, I., Siora, A., Tokarev, V., Reshetitsky, S., Bezsalyi, V, "Implementation principles of FPGA-based ESFAS for Kozloduy NPP" In: NPIC&HMIT 2009, 5–9 April, Knoxville, Tennessee.
16. Bakhmach, I., Kharchenko, V., Siora, A., Sklyar, V., Andrashov, A, "Experience of I&C Systems Modernization Using FPGA Technology", NPIC&HMIT 2010, 7–11 November, Las Vegas, Nevada, pp. 1345–1352.
17. Bakhmach, I., Kharchenko, V., Siora, A., Sklyar, V., Tokarev, V, "Design and qualification of I&C Systems on the Basis of FPGA Technologies", NPIC&HMIT 2010, 7–11 November, Las Vegas, Nevada, pp. 916–924
18. Yastrebenetsky, M., Sklyar, V., Rozen, Y., Vinogradskaya, S, "Safety assessment of FPGA-based ESFAS for Kozloduy NPP", In: NPIC&HMIT 2009, 5–9 April, Knoxville, Tennessee.
19. IEC 62566. Nuclear power plants – Instrumentation and control important to safety– Development of HDL-programmed integrated circuits for systems performing category A functions. Available at: http://webstore.iec.ch/webstore/webstore.nsf/Artnum_PK/46039
20. IAEA 2010. IAEA Review Missions of NPP I&C Systems: http://www.iaea.org/NuclearPower/Downloads/I-and-C/IERICS-Missions-2010.pdf (accessed: 10 December, 2012).
21. Bach, J., Tavolara, I, "Use of FPGA Technology in Implementation of the Logic of the Modernized Rod Control System (RCS) of the 900 MW", In: NPIC&HMIT 2010, Las Vegas, Nevada, pp. 1326–1336
22. NRC 2010b. Review Guidelines for Field-Programmable Gate Arrays in Nuclear Power Plant Safety Systems. U.S. NRC, NUREG/CR-7006, (ORNL/TM-2009/20), 2010. Available at: http://www. nrc.gov/reading-rm/doc-collections/nuregs/contract/cr7006
23. EPRI 2009. Guidelines on the use of field programmable gate arrays in nuclear power plant I&C systems. Electric Power Research Institute. Product ID: 1019181, December, 2009. Available at: http://my.epri.com/portal/server.pt?Abstract_id=000000000001019181 (accessed: 7 December, 2011).
24. EPRI 2011. Recommended approaches and design criteria for application of field programmable gate arrays in nuclear power plant instrumentation and control systems. Electric Power Research Institute. Product ID: 1022983, June 2011. Available at: http://my.epri.com/portal/server.pt?Abstract_id=000000000001022983
25. Jukka Ranta, 2012, "The current state of FPGA technology in the nuclear domain", VTT technology
26. Atkins S, Teems L, Rowe W, Selby P, Vaughters R, "Use of C-SAM acoustical microscopy in package evaluations and failure analysis", Microelectronics Reliability, Volume 38, Number 5, May 1998 , pp. 773-785

Life Cycle Reliability and Safety Engineering
Vol.3 Issue 3 (2014) 13-23

Finite Element Simulation and Optimization of Dissimilar Welding for Gas Turbine Applications

[1] V. Dillibabu, [2]Rahul V. S., [2] Muthukannan Duraiselvam
[1]Gas Turbine Research Establishment, Defense Research & Development Organization, Bangalore, India
[2]National Institute of Technology, Tiruchirappalli, Tamil Nadu, India
dilli.drdo@gmail.com

Abstract

This study uses a three dimensional finite element coupled thermo-mechanical model to simulate the laser dissimilar welding between alloy steel and nickel based super alloy using three dimensional conical Gaussian heat source and predicts the weld bead geometry, thermal gradient, cooling rate and residual stresses. Effect of laser beam power, scanning speed and laser beam offset from the interface of metals on the weld bead geometry and residual stresses are analyzed and the process is optimized.

Keywords—Laser dissimilar welding; thermo-mechanical model; finite element simulation; weld geometry; residual stress; optimization

1. Introduction

Dissimilar materials' welding is remarkably gaining attention in the industries as it can effectively increase flexibility of the design. Efficiency of the dissimilar welding strongly depends on differences in physical and chemical properties between the dissimilar materials [1]. Welding defects such as cracks, residual stresses, incomplete penetration etc. are prone to occur which calls for the necessity of optimal selection of process parameters for welding [2]. However, the advanced gas turbine technologies used in aerospace industries, make use of dissimilar joints between alloy steel and nickel superalloy because of their superior thermo-mechanical properties [3&4].

Laser welding is a high power density welding technology, which has the capability of focusing the beam power to a very small spot diameter. Its characteristics such as high precision and low and concentrated heat input, helps in minimizing the microstructural modifications, residual stresses and distortions on the welded specimens which makes it suitable for dissimilar welding [5]. Complexity in dissimilar materials welding arises due to the differences of physical and chemical properties between welding materials which may result in the less preferred residual stresses in the weldment [6]. Extensive studies on the thermal induced distortion and study on effect of process parameters are taking place in the field of laser welding. The study of laser dissimilar welding requires thermal analysis to determine depth of penetration and weld bead profile and mechanical analysis to determine residual stresses, key factor determining failure of dissimilar joints, which requires several trials before arriving at optimum conditions. Using finite element simulation and analysis effect of laser input parameters on dissimilar weld quality can be studied so that the number of trials required to arrive at optimum process parameters can be minimized which saves both time and money to a great extend. Finite Element (FE) simulation is a numerical method which can predict (and optimize) the behavior of complex laser dissimilar welding problems and analyze the thermal distribution, depth of penetration and weld bead geometry from the thermal simulation without having to rely on physically existing models, prototypes or measurements.

N Siva Shanmugam et al. [7] used a modified 3D conical Gaussian heat source for modelling laser welding. A finite element model involving moving distributed heat flux for laser transmission metal to plastic welding has been implemented by Bappa Acherjee et al. [8] into FE thermal simulations to predict temperature field during the process. Junjie Ma et al. [9] applied a three-dimensional (3D) finite element (FE) to predict the temperature evolution in the laser welding of galvanized high-strength steels in a zero-gap lap joint configuration. The effect of focal diameter, feeding rate and thermo-mechanical characteristics of the applied material, represented by its thermal diffusivity, on process efficiency in laser

micro welding is investigated by Patschger et al. [10]. An uncoupled thermo-mechanical analysis has been performed to predict the distortions and residual stresses for a single-pass fusion welded thin test plate by Abdein et al.(2009) [11]. Finite element method is used to analyze the thermo-mechanical behavior and residual stresses in laser dissimilar welding in many research works [12-15]. Many researches are undergone to determine the weld bead geometry of dissimilar laser beam butt welds and to optimize the process with respect to varying laser input parameters. However the effect of laser parameters such as beam power, welding speed, laser energy density and laser beam offset distance on dissimilar welds to optimize the process have not been studied much in detail by the researchers for optimizing the laser dissimilar welding. In this study, a three dimensional (3D) finite element (FE) coupled thermo-mechanical model is used to simulate the laser dissimilar welding between alloy steel and nickel super alloy using 3D conical Gaussian heat source which predicts the weld bead geometry, temperature gradient, cooling rate and residual stresses. Effect of laser beam power, scanning speed, energy density and beam offset from the interface of metals on the weld bead geometry and residual stresses are analyzed for process optimization. This parametric study makes use of the simulation algorithm programmed as a macro routine within the ANSYS 14.5 using ANSYS Parametric Design Language (APDL) and the adaptability of FE model is verified experimentally.

2. Theoretical Aspects

Thermal analysis

When a volume is bounded by an arbitrary surface, the balance relation of the heat flow is expressed by:

$$-\left(\frac{\partial Rx}{\partial x}+\frac{\partial Ry}{\partial y}+\frac{\partial Ry}{\partial y}\right)+Q(x,y,z,t)=\rho C\frac{\partial T(x,y,z,t)}{\partial x} \quad (2.1)$$

where R_x, R_y and R_z are the rates of heat flow per unit area, T(x,y,z) is the current temperature, Q(x,y,z) is the rate of internal heat generation, ρ is the density, C is the specific heat and t is the time. The model can then be completed by introducing the Fourier heat flow as:

$$R_x = -k_x\frac{\partial T}{\partial x} \quad (2.2.a)$$

$$R_y = -k_y\frac{\partial T}{\partial y} \quad (2.2.b)$$

$$R_z = -k_z\frac{\partial T}{\partial z} \quad (2.2.c)$$

where k_x, k_y and k_z are the thermal conductivities in the x, y and z directions, respectively. Generally, the material parameters k_x, k_y, k_z, ρ and C are temperature dependent. Inserting Eqs. (2.2.a), (2.2.b) and (2.2.c) into Eq. (2.1) yields:

$$-\left(\frac{\partial}{\partial x}\left(kx\frac{\partial T}{\partial x}\right)+\frac{\partial}{\partial y}\left(ky\frac{\partial T}{\partial y}\right)+\frac{\partial}{\partial y}\left(kz\frac{\partial T}{\partial z}\right)\right)+Q=\rho C\frac{\partial T}{\partial t} \quad (2.3)$$

Eq. (5.3) is the governing differential equation of the thermal part of the problem. The general solution is obtained by applying the following initial and boundary conditions:

$$T(x,y,z,0) = T0(x,y,z) \quad (2.4)$$

The heat transfer per unit area (QA) due to convection is expressed as:

$$QA = h(T-T_\alpha) \quad (2.5)$$

where h is the convection heat transfer coefficient and Tα is the surrounding temperature. Film coefficient is considered as independent upon temperature. Heat transfer due to radiation is not considered in this model because it not a variable and will not have significant effect in the model. Solving Eq. (2.3) by considering the boundary conditions expressed in Eqs. (2.4) and (2.5) gives the temperature distribution in the body. This temperature field will then be applied in the mechanical model to calculate the welding residual stresses and strains (distortions). In the dissimilar weld joints compared to the similar ones, the physical and mechanical properties vary in different locations of the weld joint (base material and weldment). This makes the governing equations more complicated to be solved compared to the similar joints.

The temperature fields and the evolution of the residual stresses are investigated by using finite element method. In order to accurately capture the temperature fields and the residual stresses in the weld, a 3-D finite element model is developed. The heat conduction problem is solved independently from the stress problem to obtain temperature history. However, the formulation considers the contributions of the transient temperature field to the stress analysis through the thermal expansion, as well as temperature-dependent thermo-physical properties. The material properties of both materials are assumed to be temperature dependent. All analyses are performed using the finite element analysis software ANSYS 14.5 using APDL.

Mechanical analysis

The equilibrium and constitutive equations used

here to conduct elastic–plastic mechanical analysis are described below:

Equations of equilibrium:

$$\sigma_{ij,j} + \rho b_i = 0 \quad (2.6)$$

here, σ_{ij} is the stress tensor and b_i is the body force. It is assumed that the stress tensor is symmetrical, i.e. $\sigma_{ij} = \sigma_{ji}$

Elastic–plastic constitutive equations:

$$[D\sigma] = D^{ep}\,[d\epsilon] - [C^{th}]dT \quad (2.7.a)$$

$$[D^{ep}] = [D^{e}] + [D^{p}] \quad (2.7.b)$$

where $[D^e]$ is the elastic stiffness matrix, $[D^p]$ is the plastic stiffness matrix, $[C^{th}]$ is the thermal stiffness matrix, $d\sigma$ is the stress increment, $d\epsilon$ is the strain increment and dT is the temperature increment. Since thermal elastic–plastic analysis is a non-linear problem, the incremental calculation technique is employed here in solving the problem. The incremental stress can be obtained by using the full Newton–Raphson method.

3. Finite Element Modeling

3.1 ANSYS Parametric Design Language

ANSYS Finite Element Modelling commands can be translated to create a log file with commands to model, load, solve and analyze the laser dissimilar welding. APDL stands for ANSYS Parametric Design Language, a scripting language that we can use to automate common tasks or even build our model in terms of parameters (variables). While all ANSYS commands can be used as part of the scripting language, the APDL commands are the true scripting commands and encompass a wide range of other features such as repeating a command, macros, if-then-else branching, do-loops, and scalar, vector and matrix operations. While APDL is the foundation for sophisticated features such as adaptive meshing, it also offers many conveniences that we can use in our day-to-day analyses. This finite element code is applicable for the parametric studies of a wide range of laser dissimilar welding problems with different geometrical, material and joint type, requiring only the basic thermo-mechanical material properties, geometric details, boundary conditions and laser process parameters as input. For the laser dissimilar welding, in order to study the effects of process parameters and optimize the process, APDL is most suitable finite element technique. We can record a frequently used sequence of ANSYS commands in a macro file (these are sometimes called command files). Creating a macro enables us to create our own custom ANSYS command. For example, calculating weld bead geometry after laser welding simulation in a thermal analysis would require a series of ANSYS commands in the postprocessor. By recording this set of commands in a macro, we have a new, single command that executes all of the commands required for that calculation. In addition to executing a series of ANSYS commands, a macro can call Graphics User Interface functions or pass values into arguments. The ANSYS program has many finite-element analysis capabilities, ranging from a simple, linear, static analysis to a complex, nonlinear, transient dynamic analysis. The process for a typical ANSYS analysis involves building the model, applying load, solving and reviewing the results.

Building a finite element model requires more time than any other part of the analysis. The element type used for modelling is SOLID185 which is applicable for 3-D modelling of solid structures. The alloy steel and nickel based super alloy model considered for dissimilar welding have dimensions of 25 mm length, 25 mm outer diameter and 19 mm inner diameter. This leaves a hollow tube with a thickness of 3 mm. They are kept together and meshing is done in such a way that finer meshing is adopted near the weld interface which will help us to analyze the weld bead geometry and residual stresses with increased accuracy. As shown in figure 1, for both specimens, along the thickness number of divisions taken is 6 and along length it is taken as 50 divisions for the 5mm length from the weld interface and 4 divisions for remaining 20mm. Also the circumferences of specimens are divided into 180 elements.

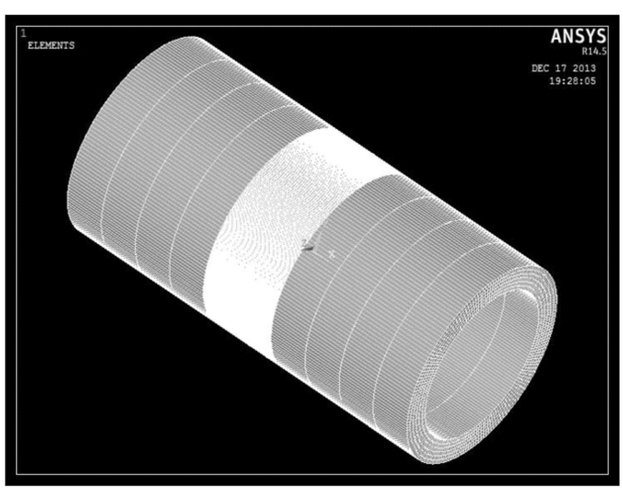

Fig. 1. Finite element model of alloy steel and nickel based super alloy

The temperature dependent material properties of both materials, as shown in figure 2 and figure 3, such as conductivity, modulus of elasticity and coefficient of linear expansion are applied to the model. Initially the two specimens will remain as separate. After welding they must be bonded at their interface. This can be ensured by defining the interface elements as contact 174 and target 170.

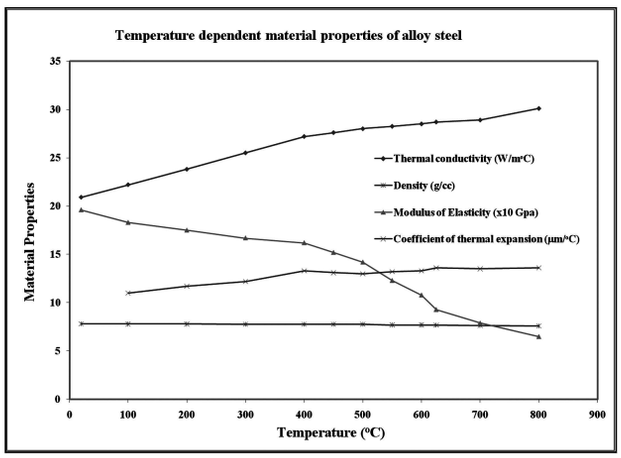

Fig. 2. Finite element model of alloy steel and nickel based super alloy

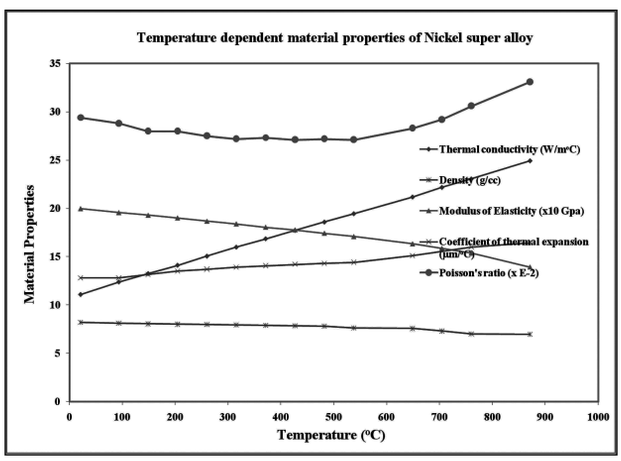

Fig. 3. Finite element model of alloy steel and nickel based super alloy

3.2 Assumptions and boundary conditions

The following points are taken into account while developing the finite element model:

- Natural convection of 15W/m^{2}K is applied over the entire surface of specimens except at the region where heat flux is applied.
- Effect of radiation on dissimilar welding is not significant as it is not a variable for the study conducted. Hence it is not considered in this model.
- Phase transformations are not considered.
- In actual process the workpiece rotate and laser head is stationary but in the proposed model it was assumed that the heat source is rotating and the workpiece are stationary.
- The initial temperature is assumed to be 25^{0}C.
- The workpiece are held at two extreme faces and in order to reduce the effect of the fixity on residual stresses, the lengths of specimens are extended to 100mm.
- Thermal properties of the material such as conductivity, specific heat, density are temperature dependent.
- There is no predefined weld bead geometry.
- It is also assumed that the laser energy is completely transferred to the base metal by direct absorption.
- Latent heat of fusion and vaporization are not considered in this model.

3.3 Heat source model

In this study, a three-dimensional conical Gaussian heat source (volumetric heat source) is used as a laser source and it is applied to specific elements in the finite element model. The modified expression for 3D conical Gaussian heat [7] source used in the analysis is given by:

$$Q = \frac{2P}{\pi r_0^2 H} e^{1-(r/r_0)^2} \left(1 - \frac{z}{H}\right) \quad (3.1)$$

where Q is the laser power intensity, r0 is the average keyhole radius, about 0.2 mm, H is the sheet thickness, r is the current radius, i.e. the distance from the cone axis, z is the vertical axis and P = η x BP, P is the absorbed laser power and BP is the beam power, and η is the efficiency, about 0.3 [7, 10].

4. Finite Element Simulation

4.1 Finite element simulation

It is possible to define the laser heat model and source centre by considering offset conditions in APDL and apply for welding the dissimilar materials. The power density values at each element Q is calculated and applied into the finite element model and moving load is implemented according to the scanning speed of laser by using the equations (4.1 and 4.2). The entire specimen is divided into 180 degrees in cylindrical coordinates and the laser heat source is fitted in such a way that the start position is at 0 degrees and it will remain over the elements in calculated time as per the scanning speed and complete the scanning at the end

of 180 load steps. The heat source is offset at 0 mm, -0.1 mm and 0.1 mm in the z-axis around the outer circumference of the specimen at the weld interface to study the effect of laser beam offset distance on quality of dissimilar laser welding. The load sub step time is calculated as per the following equation:

$$\text{Total welding time (T)} = \frac{outer\ perimeter\ of\ specimen}{scanning\ velocity} = \frac{2\pi R}{v/60} \quad (4.1)$$

$$\text{Load step time (t)} = \frac{total\ welding\ time}{load\ step\ number} = \text{T}/180 \quad (4.2)$$

where T is the total welding time in seconds(s), R is outer radius of the specimen in millimeters(mm), v is the laser scanning speed in mm/minutes. The laser heat source defined by the modified expression for 3D conical Gaussian heat source is applied on the elements at the weld interface for the calculated load sub step time. And as per the total welding time, it moves around the specimen to complete the welding.

4.2 Optimization of laser dissimilar welding

The welding parameters range chosen for the analysis is listed in the Table 1. The parameters are selected based on the expertise available at Magod laser, Bangalore, where laser welding was successfully used for many aerospace industrial applications.

Table 1 - Laser Process Parameters

Process parameters	Range Selected							
Power (W)	1550	1700	1850	2000	2150	2300	2450	2600
Speed (mm/min)	675	750	800	875	950	1000	1075	1150
Laser beam offset (mm)	0.1mm offset towards alloy steel side			No offset		0.1mm offset towards nickel based super alloy side		
Laser beam diameter	0.4 mm							

The dissimilar joint quality can be defined in terms of properties such as weld-bead geometry, depth off penetration, distortions, and residual stresses. Optimization in this study means to reduce the residual stress generation to minimum by ensuring full depth of penetration of weld. Unfortunately, a common problem faced by the manufacturer is the control of the process input parameters to obtain a good welded joint with the required bead geometry and weld quality with minimal detrimental residual stresses and distortion. Traditionally, it has been necessary to determine the weld input parameters for every new welded product to obtain a welded joint with the required specifications. To do so, requires a time-consuming trial and error development effort, with weld input parameters chosen by the skill of the engineer or machine operator. Then welds are examined to determine whether they meet the specification or not. Finally the weld parameters can be chosen after analyzing the results which of course is a time consuming and costly procedure. In this study, the laser dissimilar welding is simulated by using finite element model and the analysis is carried out to study the effect of laser welding parameters which saves a lot of time and reduces the manufacturing cost also. Since the finite element simulation is carried out using APDL macro for any process combinations the simulation can be done which simplifies the manufacturing process and optimizes the laser dissimilar welding.

5. Finite Element Analysis

The transient thermal analysis used in this study determines the temperature distribution, cooling rate and thermal gradient that vary over a period of time to identify the depth of penetration and weld bead geometry. The coupled thermo-mechanical analysis represents thermal effects coupled with residual stress generations and predicts the effect of cooling rate and thermal gradient on residual stress distribution.

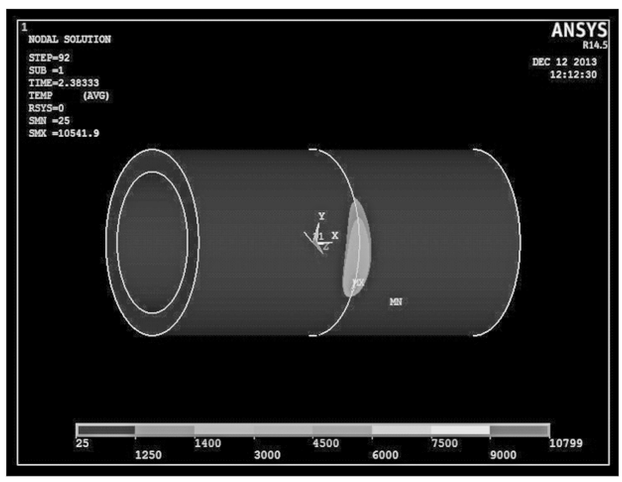

Fig. 4. Temperature distribution at 2.383s for P=2300W, V=1000 mm/min, no offset

During welding, the temperature distribution as shown in figure 4 was calculated from the thermal analysis. The bead size of each weld pass was

determined mainly according to the heat input. In the present study, the bead shape is accurately modeled by considering the melting point of both materials only. To avoid the effects of starting and ending point of welding arc, all analysis are done at points with circumferential angle equal to 180°C.

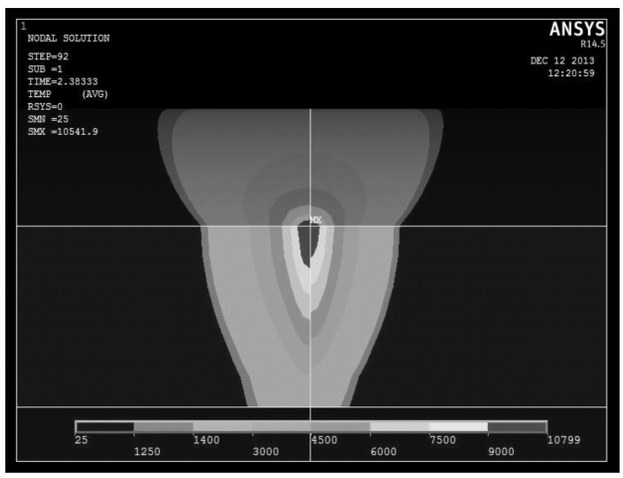

Fig. 5. Temperature distribution at 2.383 s for P= 2300W, V=1000mm/min, no offset at angle 180 degrees from start position of welding.

As shown in figure 5, we cannot directly predict the weld bead geometry from the contour thermal profile at a particular time as the laser moves. The thermal distribution is temperature dependent. Therefore we have to calculate the maximum nodal temperature at every node along depth wise and across weld interface as shown in figure 6 and compare it with the melting point of corresponding parent materials. Since we are not considering latent heat of fusion, at nodes if the maximum temperature reaches above melting point of corresponding material, the melt pool formation can be predicted which is shown in figure 7. The profile connecting nodes along depth having maximum

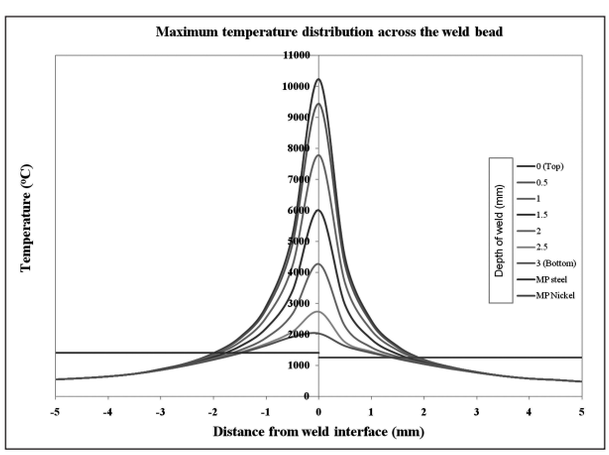

Fig. 6. Maximum temperature across the weld bead for various depth plot for P= 2300W, V=1000mm/min, no offset.

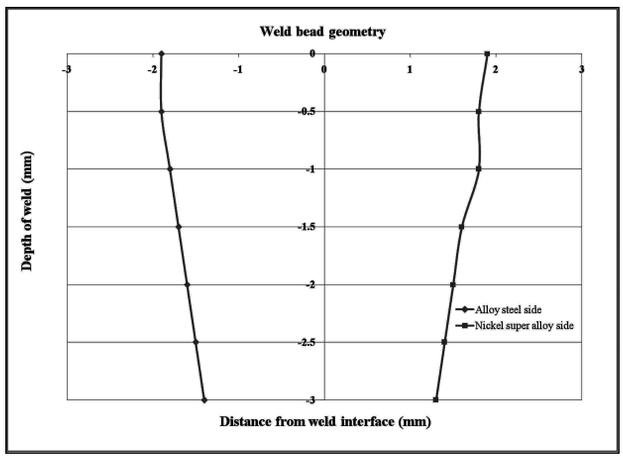

Fig. 7. Weld bead geometry calculated from Fig (6) for P=2300W, V=1000mm/min, no offset.

temperature just above melting point, results weld bead geometry.

During welding, the temperature distribution as shown in figure 5.1 was calculated from the thermal analysis. The bead size of each weld pass was determined mainly according to the heat input. In the present study, the bead shape is accurately modeled by considering the melting point of both materials only.

Cooling rate is calculated from the transient temperature distribution occurring during laser dissimilar welding by considering the following equation:

$$\frac{maximum\ temperature - reference\ temperature}{time\ taken\ to\ reach\ \max temp - time\ taken\ to\ reach\ reference\ temp} \quad (5.1)$$

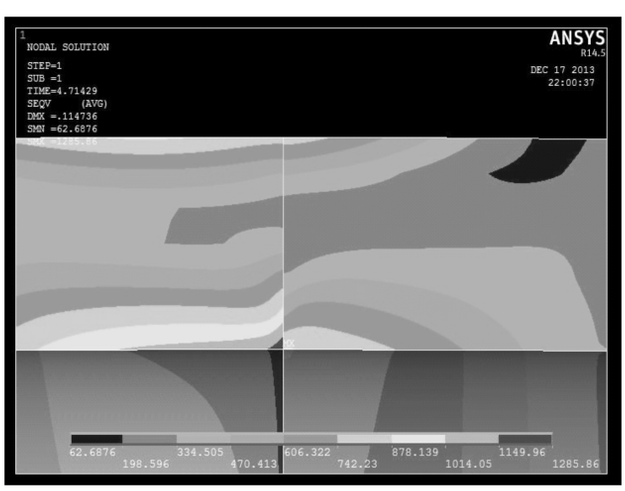

Fig. 8. Residual stress distribution at 4.71429s for P=2300W, V=1000mm/min, no offset at angle 180 degrees from start position of welding.

where reference temperature is assumed to be 1000°C. A temperature gradient is a physical quantity that describes in which direction and at what rate the temperature changes the most rapidly around a particular location. Temperature difference in any situation results from energy flow into a system or energy flow from a system to surroundings. The former leads to heating whereas latter leads to cooling of an object.

In the mechanical analysis, the temperature history obtained from the thermal analysis is input into the structural analysis as a thermal loading. Thermal stresses are then calculated at each time increment. The welding residual stresses as shown in figure 8 are the accumulated results at the final stage of the calculation, when the whole model is cooled down below 1000°C. The materials are assumed to follow the von Mises yield criterion.

6. Finite Element Model Verification

The finite element model is verified by comparing the weld bead obtained through simulation with experimentation (refer figure 9). Laser welding was performed at Magod laser, Bangalore using a 3 kW CO2 laser under argon atmosphere (flow rate -15 l/min). A suitable mandrel was prepared with an outer diameter of 19 mm which was inserted into the dissimilar pair before welding.

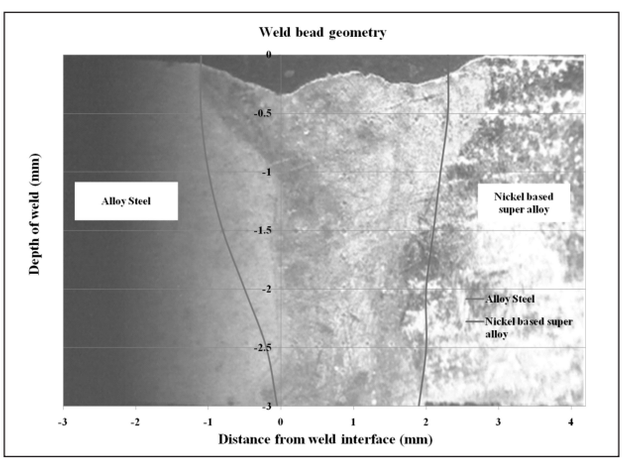

Fig. 9. Weld bead predicted by finite element simulation and obtained experimentation for P= 1700W, V=750mm/min, 0.1mm offset towards nickel based super alloy side.

In the finite element simulation model, the predicted weld bead size is more than the experimentally obtained one. The reason is that the heat energy required for latent heat of fusion is not considered. However, the weld bead profile is almost matching as it generates same trend along the depth in both sides. Variations in the weld bead geometries obtained by finite element simulation and experimentation is negligible and the finite element model is verified successfully.

7. Results and Discussions

7.1 Effect of laser power and laser scanning speed

To determine the effect of laser power and laser scanning speed on depth of penetration of weld, all other process parameters except power and speed are kept constant. Then the maximum temperature values attained at weld interface along depth, after finite element simulation of dissimilar welding for each set of laser power (refer figure 10) and speed values (refer figure 11) are plotted respectively. Along the depth at the weld interface, the maximum temperature obtained is compared with the maximum melting point value (1400°C) among the dissimilar materials. Melting does not occur where the maximum temperature value obtained during laser welding is less than 1400°C at any point along weld interface, which results only in partial weld penetration and is not acceptable. From the figure 10, it is found out that for a fixed scanning speed as power decreases, depth of penetration decreases. Depth of penetration is optimum for laser

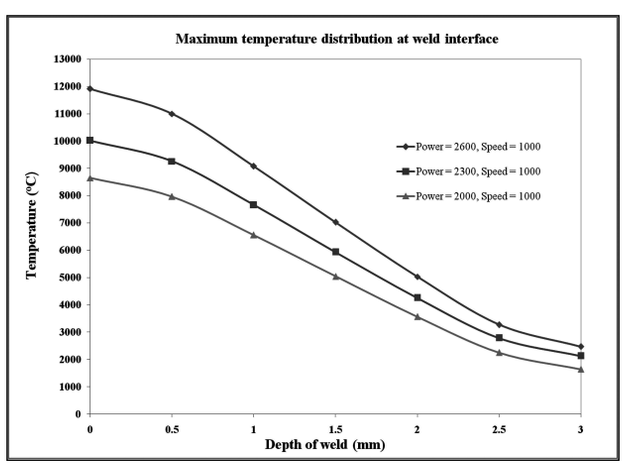

Fig. 10.Effect of laser beam power on depth of penetration.

power of 2300W and scanning speed of 1000mm/min. Also it is noted that for laser power of 2600W we are inputting more heat which may result into more thermal distortion and for laser power of 2000W, full depth of penetration is not achieved.

From the figure 11, it is found out that for a fixed power as scanning speed increases, depth of penetration decreases. Depth of penetration is optimum for scanning speed of 1000 mm/min and

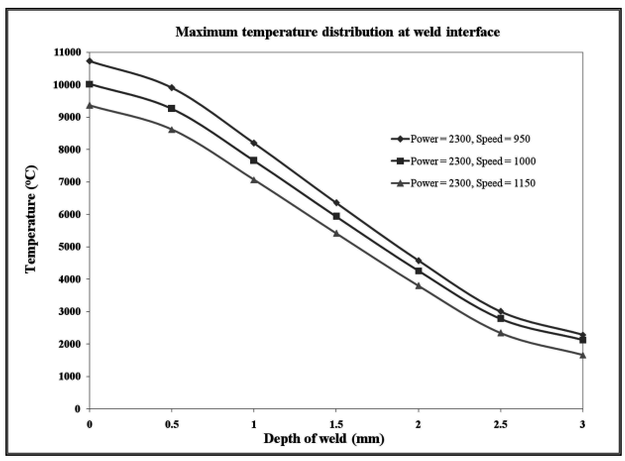

Fig. 11. Effect of laser scanning speed on depth of penetration.

laser power of 2300W. Also it is noted that for scanning speed of 950 mm/min we are inputting more heat which may result into more thermal distortion and for scanning speed of 1150 mm/min, full depth of penetration of weld is not achieved.

7.2 Effect of laser energy density

For a fixed scanning speed as power decreases depth of penetration decreases. Also for a fixed power as scanning speed increases depth of penetration decreases. Therefore it is difficult to predict the depth of penetration of weld by considering the effect of power only or scanning speed only. Hence, in order to predict the full depth of penetration, we have to consider combined effect of laser power and scanning speed i.e. energy density of laser.

$$\text{Energy density} = \text{Power density X Interaction time} \quad (7.1)$$

$$= 4P/\pi dv$$

where P is the laser power, d is the laser spot diameter and v is the laser scanning speed.

Table I. Laser energy density

Power, P (W)	Scanning speed, v (mm/min)	Laser energy density KJ/cm^2
2600	1000	49.65634
2000	1000	38.19719
2300	1000	43.92676
2300	950	46.2387
2300	1150	38.19719

Table 2 shows the laser energy density values for various power and speed combinations. Considering the optimum depth of penetration obtained for laser power of 2300W and scanning speed of 1000mm/min it can be suggested that the depth of penetration can be ensured by selecting energy density value range 43.2 -44.2 KJ/cm2. In order to verify the optimum laser energy density, consider the effect of following power and speed combination of laser with fixed energy density. Table 3 shows various laser power and speed combinations having optimum energy density values.

Table II. Different laser power and speed combinations for constant energy density

Power, P (W)	Scanning speed, v (mm/min)	Laser energy density KJ/cm2
2300	1000	43.92676
2000	875	43.65393
1700	750	43.29014

For each laser power and speed combinations as listed in table 3, the maximum temperature value attained at weld interface along depth after finite element simulation of dissimilar welding is plotted

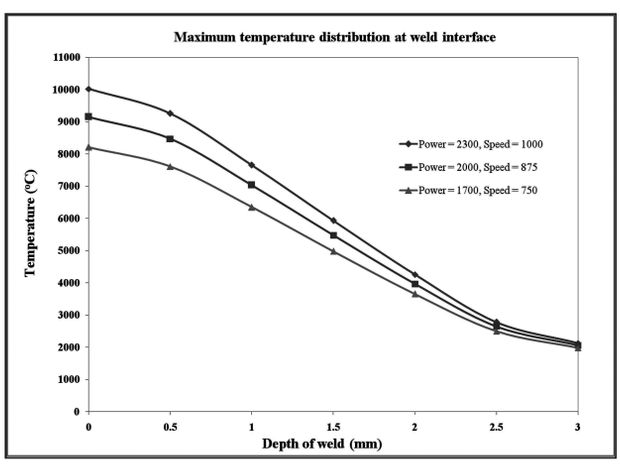

Fig. 12. Effect of laser energy density on depth of penetration.

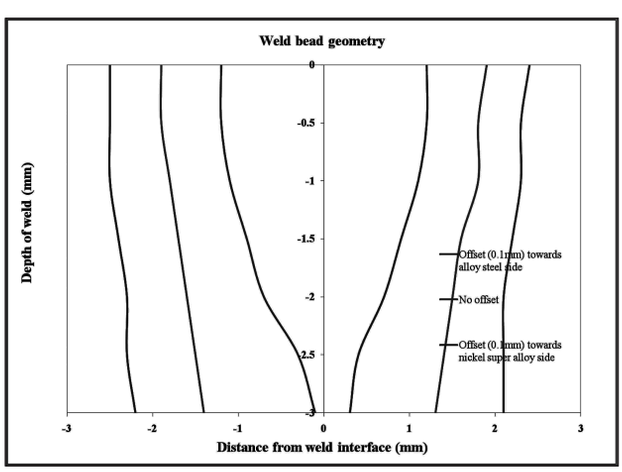

Fig. 13. Effect of laser offset distance on weld bead geometry.

(refer figure 12). From figure 12 it is observed that for each pair of combinations of laser power and speed values with fixed energy density, the depth of penetration attained is almost same and optimum. Therefore the optimum energy density which ensures full dept of penetration and without excess heat input is identified to be in the range 43.2 -44.2 KJ/cm2.

7.3 Effect of laser beam offset distance

In order to study the effect of laser offset distance, all other process parameters except laser offset distance is kept as constant. Laser power and scanning speed are taken as 2300W and 1000 mm/min for achieving full depth of penetration. Weld bead geometry is determined and along the weld bead thermal gradient, cooling rate and residual stresses are analyzed. Following are the results of the analysis done.

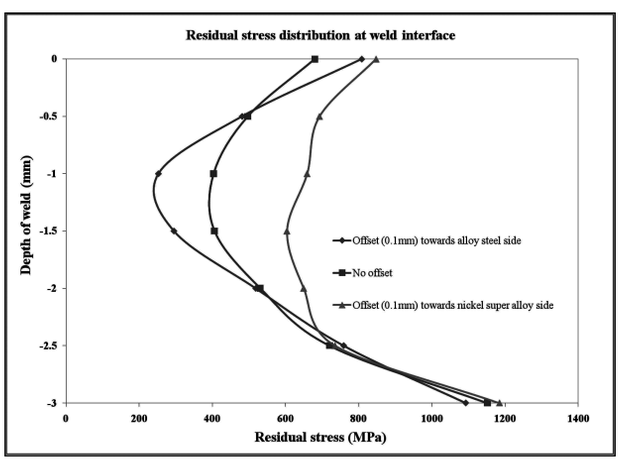

Fig. 14. Effect of laser offset distance on residual stresses.

Figure 13 shows the weld bead geometry obtained by finite element simulation of laser dissimilar welding for each set of laser beam offset distance values keeping fixed power of 2300W and laser scanning speed of 1000 mm/min. By varying the offset distance of laser focus the weld bead is found to be moving in the direction of offset. It is directly identified from the graph that offsetting more than 0.1mm towards one material may fail the melting of the other one.

In figure 14, the residual stress generation at weld interface obtained by finite element simulation of laser dissimilar welding for each set of laser beam offset distance values keeping fixed power of 2300W and laser scanning speed of 1000mm/min is shown. Considering the maximum residual stress as the failure criterion, it is occurring at the weld interface, strictly speaking, it occurs at the root side of the weld interface. Comparing the residual stresses along the weld bead and weld interface, the residual stress generation along the weld interface is much higher. So for optimization of dissimilar welding only the residual stress distribution along the weld interface is to be calculated. Now from figure 14, it is visible that at the weld interface the residual stress generation minimizes as we offset laser beam towards alloy steel side, which can be also explained by the reduced thermal gradient and cooling rate in the case of same. Therefore, from the study conducted on the effect of laser beam offset distance on dissimilar welding, the optimum offset distance is found out to be 0.1mm towards the alloy steel side.

7.4 Effect of laser power and speed combinations with fixed energy density

For the fixed optimum energy density of laser which ensures full depth of penetration, at laser offset towards the alloy steel side, the power and speed combinations are varied to determine their combined effects on weld bead geometry and residual stresses. All the study for effect of laser power and speed

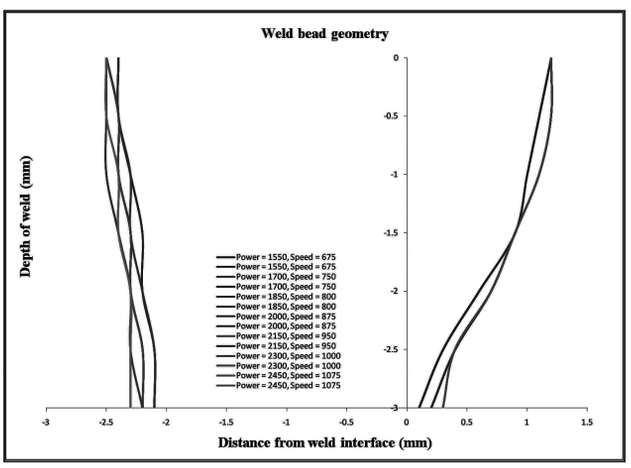

Fig. 15. Effect of power and speed combinations on weld bead.

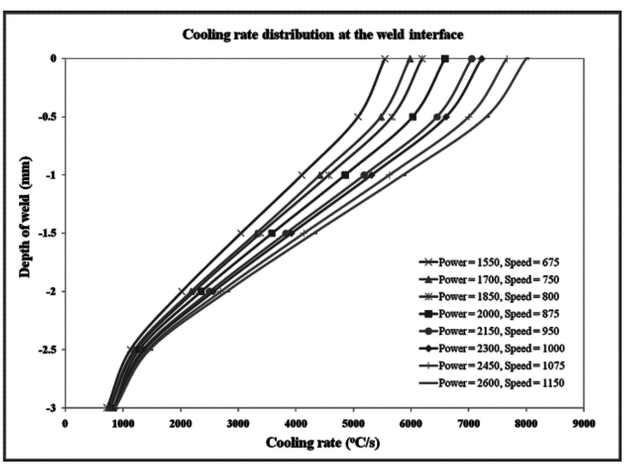

Fig. 16. Effect of power and speed combinations on cooling rate.

combinations are done at the weld interface between dissimilar materials as the cooling rate, thermal gradient and residual stress generation are observed to be maximum at this region only.

The effect of various laser power and scanning speed combinations with fixed optimum laser energy density and laser beam offset of 0.1 mm towards alloy steel side on weld bead geometry is shown in figure 15. For all laser power and scanning speed values with fixed energy density, the weld bead is similar and offset towards alloy steel side. So it is analyzed from figure 15 that the laser energy density and offset distance have significant effect on the weld bead geometry.

Figure 16 and 17 shows the cooling rate and thermal gradient distribution at the weld interface between dissimilar materials respectively for various laser power and scanning speed combinations with fixed optimum laser energy density and laser beam offset of 0.1 mm towards alloy steel side. It is observed that the cooling rate and thermal gradient values will be lower for low laser power and scanning speed combinations having same energy density and they are showing exactly identical trends throughout the depth of weld bead.

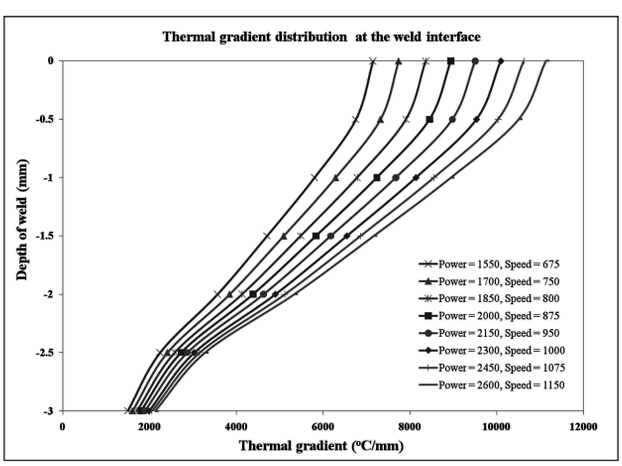

Fig. 17. Effect of power and speed combinations on thermal gradient.

Figure 18 shows the residual stress distribution at the weld interface between dissimilar materials respectively for various laser power and scanning speed combinations with fixed optimum laser energy density and laser beam offset of 0.1 mm towards alloy steel side. It is clear from the figure that the maximum residual stress values occur at the root of the weld interface. Also it is investigated from the figure 18 that on reducing the power and speed values by maintaining fixed laser energy density the residual stress generation can be minimized.

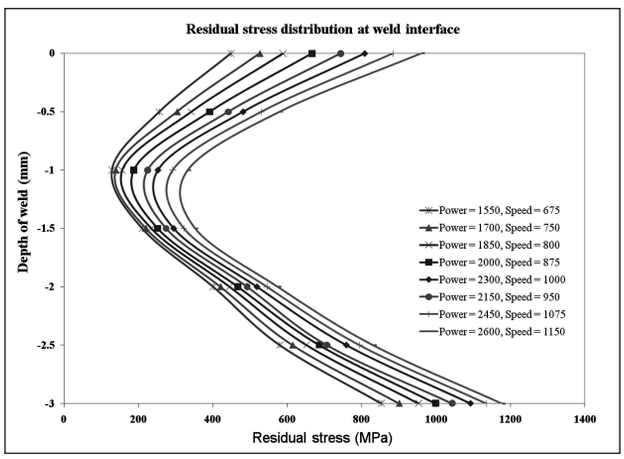

Fig. 18. Effect of power and speed combinations on residual stresses.

8. Conclusions

This study uses a three dimensional (3D) finite element coupled thermo-mechanical model to simulate the laser dissimilar welding between alloy steel and nickel based super alloy using 3D conical Gaussian heat source and predicts the weld bead geometry, thermal gradient, cooling rate and residual stresses. Effect of laser beam power, scanning speed and laser beam offset from the interface of metals on the weld bead geometry and residual stresses are analyzed and the process is optimized. Based on the results of these investigations, the following conclusions are made:

i) Laser energy density ensures depth of penetration of weld. In this study the optimized laser energy density value lies between 43.2 - 44.2 KJ/cm2.

ii) Residual stress generation reduces when the rate of cooling and thermal gradient value reduces.

iii) Residual stress generation occurs more along the interface of dissimilar materials.

iv) For a fixed power and speed combination having optimum energy density, laser beam offsetting towards alloy steel side reduces the residual stresses.

v) Residual stress generation will be lower for lower power and scanning speed combination having optimum energy density value.

vi) From the selected range of power, scanning speed and laser offset values, the optimum result can be expected at a power of 1550W, scanning speed of 675mm/min and laser beam offset of 0.1mm towards alloy steel side.

References

1. Hui Chi Chen, Andrew J. Pinkerton and Lin Li, "Fibre laser welding of dissimilar alloys of Ti-6Al-4V and Inconel 718 for aerospace applications," Advanced Manufacturing Technology, vol. 52, pp. 977–987, 2011
2. F Caiazzo, V Alfieri, V Sergi, A Schipani and S Cinque, "Dissimilar autogenous disk-laser welding of Haynes 188 and Inconel 718 superalloys for aerospace applications," Int J Adv Manuf Technol, vol. 10, pp. 013-170, 2013
3. J. Pouquet, R. M. Miranda, L. Quintino and S. Williams, "Dissimilar laser welding of NiTi to stainless steel," Int J Adv Manuf Technol, vol. 61, pp. 205–212, 2012
4. X. Liu, G. Yu, M. Pang, J. Fan, H. Wang and C. Zheng, "Dissimilar autogenous full penetration welding of superalloy K418 and 42CrMo steel by a high power CW Nd:YAG laser," Applied Surface Science, vol. 253, pp. 7281–7289, 2007
5. Yaowu Hu, Xiuli He, Gang Yu, Zhifu Ge, Caiyun Zheng and Weijian Ning, "Heat and mass transfer in laser dissimilar welding of stainless steel and nickel," Applied Surface Science, vol. 258, pp. 5914-5922, 2012
6. H. Serizawa, D. Mori, Y. Shirai, H. Ogiwara and H. Mori, "Weldability of dissimilar joint between F82H and SUS316L under fiber laser welding," Fusion Engineering and Design, 2013
7. Siva Shanmugam N, Buvanashekaran G, Sankaranarayanasamy K and Ramesh Kumar S, "A transient finite element simulation of the temperature and bead profiles of T-joint laser welds," Materials and Design, vol. 31, pp. 4528-4542, 2010
8. Bappa Acherjee, Arunanshu S. Kuar, Souren Mitra and Dipten Misra, "Finite element simulation of laser transmission welding of dissimilar materials between polyvinylidene fluoride and titanium," International Journal of Engineering, Science and Technology, vol. 2, pp. 176-186, 2010
9. Junjie Ma, Fanrong Kong and Radovan Kovacevic, "Finite-element thermal analysis of laser welding of galvanized high-strength steel in a zero-gap lap joint configuration and its experimental verification," Materials and Design, vol. 36, pp. 348–358, 2012
10. A. Patschger, J. Bliedtner and J. P. Bergmann, "Approaches to increase process efficiency in laser micro welding," Physics Procedia, vol. 41, pp. 592 – 602, 2013
11. Muhammad Zain-ul-Abdein, Daniel Nelias, Jean-Francois Jullien and Dominique Deloison, "Prediction of laser beam welding-induced distortions and residual stresses by numerical simulation for aeronautic application," Journal of materials processing technology, vol. 209, pp. 2907-2917, 2009
12. D. Akbari and I. Sattari-Far, "Effect of the welding heat input on residual stresses in butt-welds of dissimilar pipe joints," International Journal of Pressure Vessels and Piping, vol. 86, pp. 769-776, 2009
13. M. Peric, Z. Tonkovic, A. Rodic, M. Surjak, I. Garašic, I. Boras and S.o Švaic, "Numerical analysis and experimental investigation of welding residual stresses and distortions in a T-joint fillet weld," Materials and Design, vol. 53, pp. 1052–1063, 2014
14. P. Chang and T Teng, "Numerical and experimental investigations on the residual stresses of the butt-welded joints," Computational Materials Science, vol. 29, pp. 511–522, 2004
15. E.M. Anawa and A.G. Olabi, "Control of welding residual stress for dissimilar laser welded materials," Journal of materials processing technology, vol. 204, pp. 22–33, 2008

Life Cycle Reliability and Safety Engineering
Vol.3 Issue 3 (2014) 24-31

Inter Comparison of REPAS and APSRA Methodologies for Passive System Reliability Analysis

[1]RB Solanki, [2]Suneet Singh, [3]P. V. Varde, [4]A. K. Verma, [1]P. R. Krishnamurthy
[1]Atomic Energy Regulatory Board, Mumbai, India, [2]Indian Institute of Technology, Mumbai, India,
[3]Bhabha Atomic Research Centre, Mumbai, India, [4]Stord/Haugesund University College, 5528, Haugesund, Norway,
rajsolanki@aerb.gov.in

Abstract

The increasing use of passive systems in the innovative nuclear reactors puts demand on the estimation of the reliability assessment of these passive systems. The passive systems operate on the driving forces such as natural circulation, gravity, internal stored energy etc., which are moderately weaker than that of active components. Hence, phenomenological failures (virtual components) are equally important as that of equipment failures (real components) in the evaluation of passive system reliability.

The contribution of the mechanical components to the passive system reliability can be evaluated in a classical way using the available component reliability database and well known methods. On the other hand, different methods are required to evaluate the reliability of processes like thermal-hydraulics due to lack of adequate failure data. The research is ongoing worldwide on the reliability assessment of the passive systems and their integration into PSA, however consensus is not reached.

Two of the most widely used methods are Reliability Evaluation of Passive systems (REPAS) and Assessment of Passive System Reliability (APSRA). Both these methods characterize the uncertainties involved in the design and process parameters governing the function of the passive system. However, these methods differ in the quantification of passive system reliability.

Inter comparison among different available methods provides useful insights into the strength and weakness of different methods. This paper highlights the results of the thermal hydraulic analysis of a typical passive isolation condenser system carried out using RELAP mode 3.2 computer code applying REPAS and APSRA methodologies. The failure surface is established for the passive system under consideration and system reliability has also been evaluated using these methods. Challenges involved in passive system reliabilities are identified, which require further attention in order to overcome the shortcomings of these methods. These procedures can then be applied for evaluating passive system reliability, which would be used in risk-informed decision-making.

Key words: Passive systems, Reliability analysis, Reliability Evaluation, REPAS, Assessment, APSRA, risk-informed decision making

1. Introduction

The increasing use of passive systems in the innovative nuclear reactors puts demand on the estimation of the reliability assessment of these passive systems. The passive systems operate on the driving forces such as natural circulation, gravity, internal stored energy etc., which are moderately weaker than that of active components. Hence, phenomenological failures (virtual components) are equally important as equipment mechanical failures (real components) in case of passive system reliability evaluation.

The contribution of the mechanical components to the passive system reliability can be evaluated in a classical way using the available component reliability database and well known methods. On the other hand, different methods are required to evaluate the reliability of thermal-hydraulic process due to lack of adequate failure data. The research is ongoing worldwide on the reliability assessment of the passive systems and their integration into PSA, however consensus is not reached.

Literature survey indicates that there are many methods that were developed for assessment of passive system reliability [1, 2, 3, 4, 5, 6]. However, consensus is not yet reached. Reliability Evaluation of Passive systems (REPAS) [7, 8, 9] and Assessment of Passive System Reliability (APSRA) methods [10, 11] are most popular among these methods.

In this paper, the inter-comparison of RMPS and APSRA methodology is carried out on a common passive safety system. The methodology, results and insights are discussed. Challenges involved in passive system reliabilities are identified, which require further attention in order to overcome the shortcomings of these methods.

2. Brief Description of REPAS Methodology

This section describes two widely used approaches for passive system reliability assessment (i.e. REPAS and APSRA).

The REPAS characterizes the performance of passive systems in an analytical way. Therefore, the methodology may provide numerical values that can be used in more complex safety assessment study and might be seen as the equivalent of the 'Fault-Tree' analysis that is used as a support for a probabilistic safety assessment (PSA) study. The major procedural steps of REPAS methodology are given here.

i) Step 1: Characterization of design / operational status for the system

The mission of the system and relevant phenomenology involved in the system should be identified. The design parameters (like pressure, level, temperature etc.) and critical parameters (like presence of non-condensable gases, heat losses in piping etc.), which govern the system should be identified. The full characterization of T-H systems requires large number of parameters. Experts' judgment could be used to identify the optimum system parameters.

ii) Step 2: Definition of failure criteria for the system performance

The failure criteria for the system performance can be derived from the knowledge of the mission of the system. The failure criteria can be established as single-value targets (e.g. failure to deliver a specific quantity of liquid within a fixed time) or as a function of time targets.

iii) Step 3: Computer code modeling

The experimental database for the operation of the T-H passive systems is sparse. Hence, for performance evaluation of the T-H system, one has to rely upon the numerical modeling through best-estimate computer codes. The system analysis should be done with validated T-H computer codes and performing best-estimate calculations.

iv) Step 4: Assigning probability distributions to Design and Critical parameters

The nominal values and the range for the design and critical parameters must be identified as a part of system characterization. The probability distributions for the occurrence of that value of the parameters are assigned in this task. This can be done through experts' judgment, possibly taking into account available data on operation and maintenance of the T-H passive systems. Once the ranges and associated probabilities are fixed, a stochastic selection of a limited number of system configurations is performed through Monte-Carlo procedure.

v) Step 5: Deterministic evaluations of stochastic system configuration set

Through stochastic selection of the system configurations, a set of accident and operational transients is performed with best-estimate T-H computer codes with different initial values for the design and critical parameters. The stochastic selection of system configurations and corresponding output set represents the general physical behavior of the passive system.

vi) Step 6: Deterministic evaluations of deterministic system configuration set

The system configurations judged of particular interest by experts also needs to be included in the analysis for the overall performance evaluation of the T-H passive systems. These configurations would be the non-nominal initial conditions (e.g. presence of significant amount of non-condensable gases, "extreme" cases with concurrent non-nominal values of different parameters) with which system has to perform its intended function within the mission time.

vii) Step 7: Quantitative reliability evaluation

The analysis results obtained from the computer code runs are quantitatively analyzed by applying failure criteria defined in step 2. From the analysis results, the T-H passive system failure probability can be calculated using different method like direct Monte-Carlo, Monte-Carlo with response surface method etc.

3. Brief Description of APSRA Methodology

To overcome the difficulties in assigning the arbitrary probability distribution functions, a different approach is developed for passive system reliability assessment based on APSRA methodology [14, 15]. The major procedural steps of APSRA methodology are given here.

i) **Step1: Identification of Passive system to be evaluated**

The passive system for which reliability will be evaluated is identified.

ii) **Step 2: Identification of parameters affecting the operation**

The performance of passive system may be affected by many parameters. This can be examined qualitatively considering the effect of these parameters on the performance.

iii) **Step 3: Operational characteristics and failure criteria**

Under normal operating conditions, system parameters are steady and may deviate within the operating range due to overall system dynamics. During the abnormal conditions, the position of some components of the system changes in response to the transients and corrective actions are taken to limit the deviations within the safety limits of key parameters.

iv) **Step 4: Key parameters which may cause the failure**

The performance of passive system may be affected by many parameters. However, the system operation is more sensitive to certain parameters than others. This can be examined considering the effect of these parameters on the performance through detailed thermal hydraulic analyses.

v) **Step 5: Generation of failure surface and validation with test data**

Deviation of the critical parameters from their nominal value is considered and system behavior is predicted using a best estimate code RELAP5/Mod 3.2 [16]. This requires analysis for various combinations of critical parameters. The system behavior in terms of success/failure is represented in a parametric space and a failure surface demarcating the failure and the success regions is generated.

vi) **Step 6: Root diagnosis to find deviation of key parameters causing ultimate failure of system**

After establishing the domain of failure, the nest task is to find out the cause of deviation of key parameters which eventually result in the failure of the system. Different fault trees are developed for different key parameters.

vii) **Step 7: Evaluation of failure probability of components causing the failure**

The failure probabilities of the components that have been identified as root causes have been obtained from the generic data values or plant-specific failures.

viii) **Step 8: Evaluation of passive system Reliability**

Using the component failure probabilities obtained in the previous step, system reliability analysis is performed for obtaining the system failure probability using the fault tree analysis method.

4. Isolation Condenser System

Isolation Condenser (IC) system currently being used in most of the innovative NPPs is considered for performance evaluation using APSRA and REPAS methods. The system is categorized as category-D type as per IAEA classification scheme [12]. The safety function depends on the principle of natural circulation (passive means) except that internal "intelligence" of actuation signal is not available in this system. At a pre defined set point, valves opens automatically. The system is illustrated in Fig. 1. The

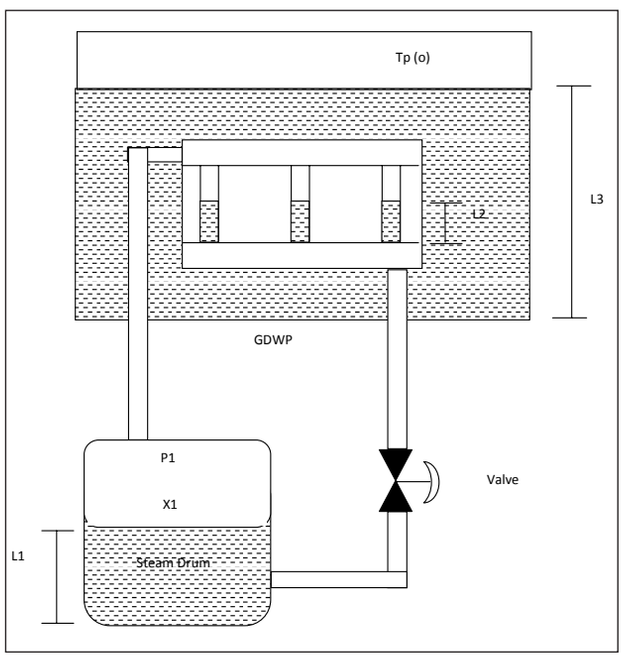

Fig. 1 Isolation Condenser System

system consists of Steam Drum (SD), heat exchanger, also known as Isolation Condenser (IC), a discharge valve in the return path of IC and associated piping. The IC is immersed in a large water pool, also known as Gravity Driven Water Pool (GDWP).

On opening of the valve, the system operates on two-phase natural circulation principle. The GDWP and IC are at higher elevation than the power source (i.e. SD). The objective of the system is to reject the core decay heat produced after reactor shutdown to the heat sink (GDWP) by condensing the primary fluid (steam) into the heat exchanger tube bundles (IC tubes).

5. Reliability Assessment Using REPAS Methodology

The system is characterized using the design and critical parameters. The design parameters are the governing parameters. The critical parameters are those, which can affect the heat transfer capability and the natural circulation flow rates. The main design parameters identified are: Steam Drum pressure (P1), the liquid level in the steam drum (L1), the liquid level in GDWP (L3) and the GDWP temperature (Tp). The main critical parameters identified are: presences of non-condensable gases in Steam drum (X1) and the liquid level in IC tubes (L2). The probability distribution is assigned to these parameters for simulating different system configurations. This are indicated in Table 1 and Table 2.

For assigning the probability to the discrete initial parameter values, experts' judgment is used. The nominal value of the parameter is the most probable value expected for the operation of isolation condenser system. This is a pivot around which the probability of the other discrete parameter values can be assigned suitably on either side. The probability values are assumed to be decreasing towards to lower and upper limit of the ranges.

The RELAP5 mode 3.2 computer code is used for the deterministic analysis of the system behavior under different system configurations. The computer code takes lot of computational time for detailed calculation of various thermal-hydraulic properties (i.e. pressure, temperature etc.). In order to make the evaluation feasible, a limited but statistically meaningful number of system configurations should be selected for actual computer runs.

The Wilks formula has been adopted to determine the adequate sample size using fractile value α and confidence level β [13, 14]. For two-sided statistical tolerance intervals the formula is:

Table 1 Design Parameters of Isolation Condenser system

Design Parameters	Unit	Nominal Value	Range	Discrete Initial Values and probabilities					
SD Pressure (P1)	Bars	76.5	70-86	70.0	73.0	76.5	83.0	86.0	value
				0.01	0.03	0.90	0.04	0.02	pdf
SD water Level (L1)	m	2.165	0.6-3.0	0.8	1.5	2.0	2.165	3.0	value
				0.01	0.02	0.07	0.85	0.05	pdf
GDWP water Level (L3)	m	5.0	3.0-5.0	3.13	3.50		4.48	5.0	value
				0.01	0.04		0.05	0.9	pdf
GDWP initial temperature (Tp)	°C	40	35-60	35	40	50	60		value
				0.1	0.85	0.03	0.02		pdf

Table 2 Critical Parameters of Isolation Condenser system

Critical Parameters	Unit	Nominal Value	Range	Discrete Initial Values and probabilities							
Non-condensable gas fraction in SD (X1)		0.0	0-1	0.00	0.01	0.10	0.20	0.30	0.40	0.50	value
				0.80	0.10	0.05	0.03	0.01	0.006	0.004	pdf
IC Tube water Level (L2)	%	100	0-100	50.0		80.0		100			value
				0.03		0.07		0.90			pdf

$$1-\alpha^N - N(1-\alpha)\alpha^{N-1} \geq \beta$$

It is found that for two-sided tolerance interval, one can affirm with 80 % confidence coefficient that the output parameter would bound at least 90% of the population by using 30 system configuration runs.

To assess the system performance, the success criteria needs to be established first. In the present case study, the heat rejection capability of the isolation condenser system is considered as a parameter of interest during the reactor shutdown.

The ratio (Integral power ratio) of cumulative heat rejected in a particular system configuration during the mission time and the same in a nominal configuration has been chosen as the failure criteria for the isolation condenser system performance evaluation.

$$\text{Integral Ratio} = \int_0^t \dot{W}_2\, dt \Big/ \int_0^t \dot{W}_{2\,No\,\min al}\, dt$$

If the falls below a fixed fraction of that of the "nominal" configuration, it would be considered as system failure. The time evolution of the integral power ratio during the mission time has been shown in Fig. 2 for different system configurations.

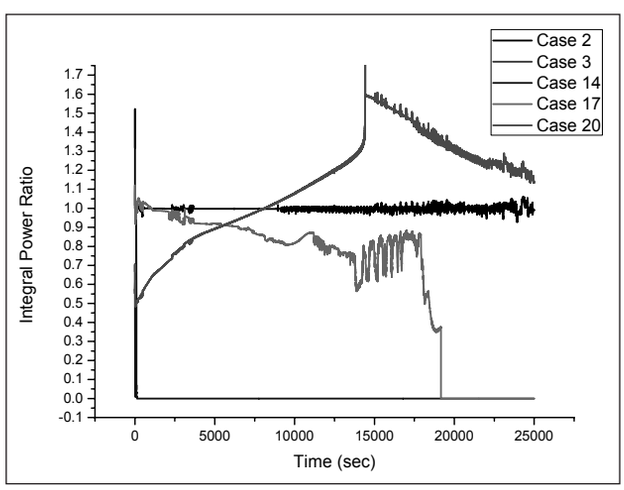

Fig. 2 Integral power ratio variation in representative system configurations

To get the adequate sample size for realistic reliability evaluation of isolation condenser system, an approximate mathematical model called "Response Surface" has been developed. For simplicity, the linear response surface model using the multiple regression with six independent parameters (i.e. P1, L1, L3, Tp, X1 and L2) and one dependent parameter (integral power ratio) have been adopted. Using the RELAP code results for 30 cases, the regression coefficients have been calculated using the linear multiple regression method.

The following linear "response surface" model was obtained:

$$\text{Integral power ratio} = B_o + B_1 * P_1 + B_2 * L_1 + B_3 * L_3 + B_4 * T_p + B_5 * X_1 + B_6 * L_2$$

To get true failure probability, one should have adequate (large) sample size. Hence, total 1,00,000 Monte-Carlo simulations have been performed using the "response surface" model. The reliability of the isolation condenser system has been evaluated in terms of the failure probability of the system. For the present case, this works out to be 1.002E-01.

6. Reliability Assessment Using APSRA Methodology

After identifying the governing parameters, the performance of ICS is evaluated by changing the initial values of some of the important parameters, which are vital for system performance. The system performance is affected by many parameters such as presence of non-condensable (NC) in steam drum, decrease in water level of the pool, rise in the temperature of water pool etc.

Water level in the GDWP pool is maintained by a make-up system with a heat exchanger that maintains the water temperature. Similarly, the water level in steam drum is maintained by feed water system.

The system performance is evaluated against the same failure criteria used in REPAS methodology (i.e. integral power ratio).

By keeping all other parameters at their nominal values, a single parameter is varied and system performance is evaluated using the computer code

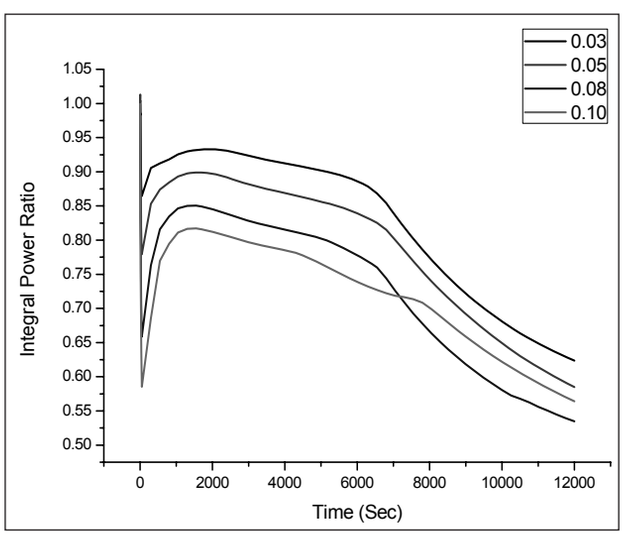

Fig. 3 Effect of Non-Condensable in steam drum

RELAP. The system behavior in terms of success/ failure is represented in a parametric space and the failure surface is generated.

For comparing the system performance relatively during different initial condition of critical parameter, first a base case scenario is analyzed as done in REPAS methodology.

Non-Condensable is assumed to be present in the steam drum for the analysis. Fig. 3 indicates the variation of integral power ratio during the mission time for different amount of non-condensable (i.e. ranging from 3% to 10%). It can be seen that integral power ratio increases initially and starts decreasing towards the end of the mission time of 8000 seconds. This is due to the degraded conditions in ICS (mismatch between core decay power and IC heat rejection to GDWP). Steam drum pressure continuously reduces due to poor condensation of steam inside the IC tubes.

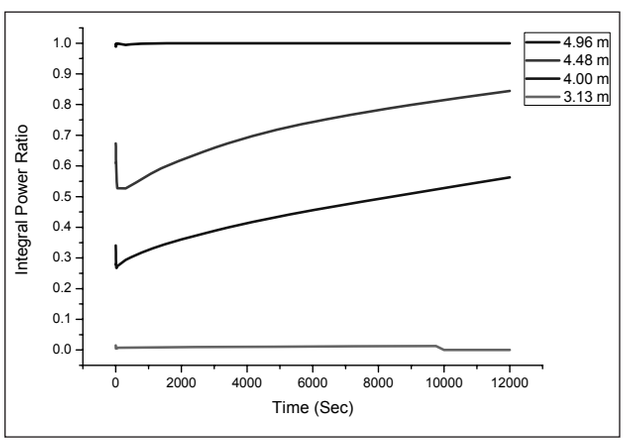

Fig. 4 Effect of GDWP water level

The condenser tubes are normally submerged in the large pool of water contained in GDWP. If the water level in GDWP goes down due to evaporation or failure of the make-up system, these condenser tubes get exposed. As the tubes are getting exposed, less surface area remains for steam condensation. The steam drum pressure starts rising. Fig. 4 indicates the variation of integral power ratio during the mission time with different GDWP water level. It can be seen that as the GDWP level reduces, the integral power ratio drops below the success criteria established for the system performance evaluation.

During the normal condition, WDWP temperature is maintained at around 40 ^{0}C. The GDWP temperature is assumed to vary for the analysis. Fig. 5 indicates the variation of integral power ratio during the mission

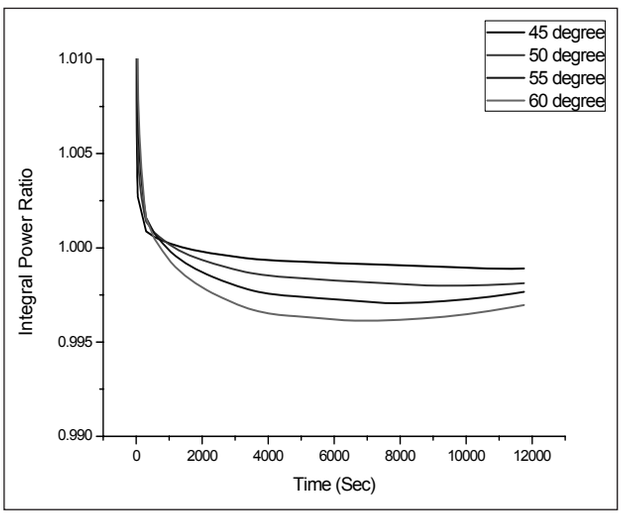

Fig. 5 Effect of water temperature of GDWP

time for different GDWP water temperatures (i.e. ranging from 45 ^{0}C to 60 ^{0}C). It can be seen that integral power ratio decreases initially and then remains steady between 0.8 to 1.0 from the mission time of 2000 seconds.

It was found that heat transfer condition has rather improved due to local boiling in the pool near the condenser tube surface. This results in to the higher heat transfer coefficient due to nucleate boiling in pool near top of IC tubes.

The failure surface provides the limiting condition of critical parameters governing the system performance. Once the failure surface is established, the next task is to identify the attributes for deviation in the key governing parameters, which eventually lead to system failure. For quantifying the reliability of the passive system, the likelihood of process parameters attaining values such that the operating condition lead to degrading condition to the extent of crossing the failure surface needs to be assessed.

Fault tree analysis technique is used for modeling this aspect. For quantitative assessment of reliability, the failure probabilities need to be assigned to each of the components appearing into the fault tree as basic events. Generic data from IAEA TECDOC-478 [15] are used as an illustration purpose in this paper. The Fault tree for the Isolation Condenser system is shown in Fig. 6. Risk Spectrum computer code is used for modeling and quantification of system reliability. While the probability of low water level in GDWP is worked out based on the failure probability of make-up system, the probabilities of the presence of non-condensable gases in steam drum and GDWP temperature high are assumed to be 1.0E-04. The

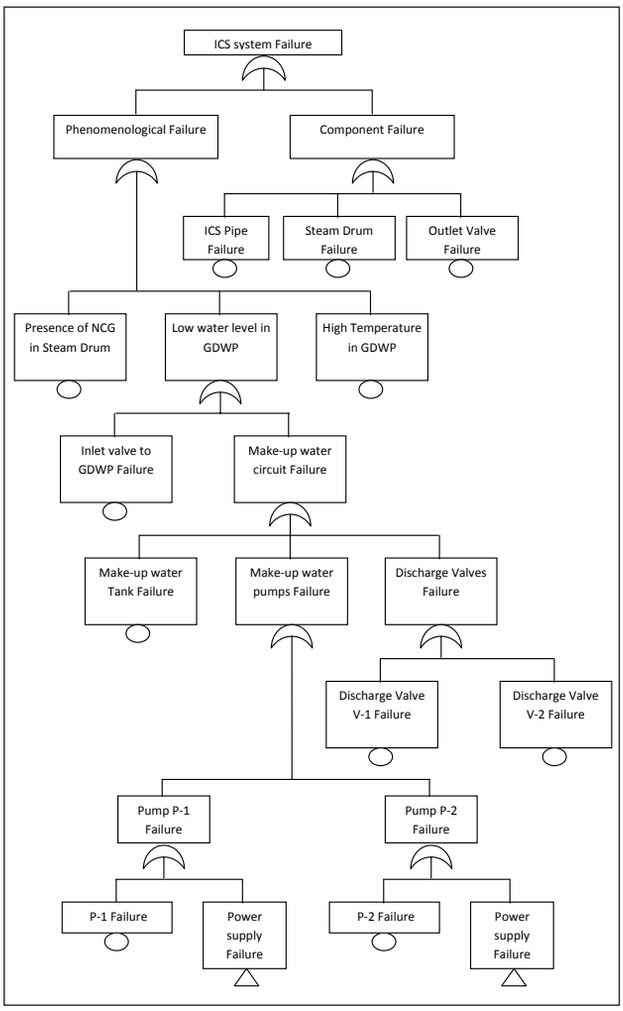

Fig. 6 ICS Fault tree

system reliability is expressed in terms of system unavailability. This works out to be 2.200E-03.

7. Results and Insights

REPAS methodology is based on estimating the reliability through parametric uncertainty analysis. To address the issue of large computation time it relies on the Wilk's theory of finding out the optimum number of computer code runs for a given confidence level. Using the results of these limited code runs, a response surface (mathematical model) is generated, which is used to predict the parameter of interest for different system configurations. The system reliability is estimated in terms of failure probability. In the current case study this works out to be 1.002E-01.

Parametric uncertainty analysis is well established approach; however, the selection of probability function and associated probability values to the parameters is subjective. Further, the response surface is derived through multivariate regression of the limited computer code results; the failure probability does not really change substantially by performing large number of simulations through identified response surface to predict system performance.

APSRA methodology is based on estimating the system reliability through classical fault tree approach. The parameters of interests are identified through parametric studies on computer code by analyzing system performance under different values of these parameters. Through root cause approach, the mechanical components in the system are identified, the failure of which could be attributed for deviations during the mission time, which eventually leads to system failure under degraded condition. These failures of the components are modeled in the fault tree. The fault tree analysis is carried out using Risk Spectrum computer code. The system reliability is expressed in terms of system unavailability. This works out to be 2.2E-03.

The system unavailability is estimated using the classical fault tree approach, in which the phenomenological failures are identified due to critical parameters. However, the probabilities of such parameters attaining values such that the system does not fulfill its intended function are not derived from systematic process but subjectively assumed. Both these methods adopt different approaches in estimating the system reliability. Both methods rely on subjective assignment of probabilities at some stage of the process.

8. Conclusion

REPAS and APSRA methodologies are complementary to each other. While REPAS is based on parametric uncertainty analysis, APSRA on the other hand is based on classical fault tree approach. There is a scope for improving up on the short coming of these methods and developing a method in which the subjective elements is reduced if not completely eliminated. Moreover, these methods are applied on different systems and on limited scale also there is very little operating experience on the passive system performance. Hence, the validation of these methods remains an open issue.

Integration of passive system reliability assessment methods with Probabilistic Safety Analysis (PSA) also requires a different approach as the passive system performance depends on the process parameters, which may change during the mission. Dynamic event trees would be required to capture the changing

process parameters influencing the passive system performance.

References

1. F. Bianchi, L. Burgazzi, F. D. Auria, M. E. Ricotti, "The REPAS approach to the evaluation of Passive Safety Systems Reliability", NEA/CSNI/R(2002)10, pp. 133-148, 2002.
2. M. H. Prasad, A. J. Gaikwad, A. Srividya, A. K. Verma, "Failure probability evaluation of passive system using fuzzy Monte Carlo simulation, Nuclear Engineering and Design", pp. 1864-1872, 2011.
3. International Atomic Energy Agency, IAEA-TECDOC-1624, "Passive Safety Systems and Natural Circulation in Water Cooled Nuclear Power Plants", November 2009.
4. International Atomic Energy Agency, IAEA-TECDOC-920, "Technical feasibility and Reliability of Passive Safety Systems for Nuclear Power Plants", December 1996.
5. L. Burgaazi, "Addressing the uncertainties related to passive system Reliability", Nuclear Energy, pp. 93-102, 2007.
6. Durga Rao K, et al., "Quantification of epistemic and aleatory uncertainties in Level-1 probabilistic safety assessment studies", Reliability Engineering and System Safety, pp. 947–56, 2007.
7. M. E. Ricotti, M.E., Zio E., D'Auria F., Caruso G., "The REPAS Study: Reliability evaluation of Passive Safety Systems, International Conference on Nuclear Engineering", ICONE-10, Arlington, Virginia, USA, 2002.
8. J. Jafari, F. D' Auria, et. al, "Passive system reliability analysis: a study of the isolation condenser", Nuclear Technology, pp. 3-9, 2002.
9. L. Burgaazi, "Addressing the challenges posed by advanced reactor passive safety system performance assessment", Nuclear Engineering and Design, pp. 1834-1841, 2011.
10. A. K. Nayak, M. R. Gartia, A. Antony, G. Vinod, and R. K. Sinha, "Passive system reliability analysis using APSRA methodology", Nuclear Engineering and Design, pp. 1430-1440, 2008.
11. A. K. Nayak, Vikas Jain, M. R. Garita, Hari Prasad, A. Anthony, S. K. Bhatia, R. K. Sinha, "Reliability assessment of passive isolation condenser system of AHWR using APSRA methodology", Reliability Engineering and System Safety, pp. 1064–1075, 2009.
12. INTERNATIONAL ATOMIC ENERGY AGENCY, "Safety Related Terms for Advanced Nuclear Power Plants", TECDOC-626, 1991.
13. Report on "Support methods for Estimating the Reliability of Passive systems", Deliverable 4, RMPS Project, 2002.
14. Wilks S. S., "Determination of sample sizes for setting tolerance limits", Annals of Mathematical Statistics, 12, pp. 91-96, 1941.
15. INTERNATIONAL ATOMIC ENERGY AGENCY, "Component Reliability data for use in Probabilistic Safety Assessment", IAEA-TECDOC-478, 1988.

Life Cycle Reliability and Safety Engineering
Vol.3 Issue 3 (2014) 32-41

Reliability Analysis of Reinforced Concrete Bridge piers subjected to Earthquakes

K. Balaji Rao, M.B. Anoop
CSIR-Structural Engineering Research Centre, CSIR Campus, Taramani, Chennai, India
balaji@serc.res.in

Abstract

A practical method for the determination of reliability of bridge pier (carrying a concentrated mass at the top and idealized as a single degree freedom system) subjected to stochastic seismic excitation is presented in this paper. The methodology developed is based on Monte Carlo simulation technique. Using this methodology the probabilities of failure of a model of a prototype bridge pier (whose test results are reported by Hachem et al. [1]) against the limit states of serviceability and damage control have been determined. In the reliability analysis, the system parameters namely, mass, stiffness, restoring force and damping coefficient are treated as lognormal variables and, the seismic excitation (which is a scaled down version of North Ridge earthquake) is treated as stochastic. The limiting tip displacements corresponding to various limit states of the nominal structure are obtained from the moment-curvature and shear force-displacement analysis. Treating these as the nominal allowable values for the pier considered, the probabilities of failure are determined by posing the problem as a first passage problem. Also, the statistical properties of the time to reach the limit states are presented in this paper.

Keywords: non-linear SDOF system response; stochastic seismic excitation; reinforced concrete bridge pier; serviceability limit state; damage control limit state; reliability analysis

1. Introduction

Reliability analysis of bridge piers subjected to stochastic seismic excitation has been carried out by many researchers in the past. Generally, this problem is posed as a random vibration problem and the solution is obtained for first passage time. Also, assumptions are made regarding the system behaviour (in most studies system is considered to be linearly elastic) and the excitation to be stationary white noise excitation or filtered and/or modified white noise excitation (viz. Köyluoglu et al. [2] and the references therein). Most of these studies are not directly applicable for reinforced concrete bridge piers since the reliability analysis method should identify the fact that the limit states are defined with respect to the limiting values of ductility (curvature or displacement) and the system behaviour can be nonlinear even at the end of serviceability limit states. This indicates that there is a need to consider the input excitation as band limited non-white excitation and system response should be evaluated taking into account the possible nonlinear behaviour.

Akiyama *et al.* [3] carried out a reliability analysis of RC bridge piers designed according to three different editions of seismic codes of Japan. They carried out a sensitivity analysis to identify important uncertain variables, involved in the design, contributing to the failure probability of bridge pier. The limit states considered included shear failure, ductility, and the residual displacement. One of the important conclusions was that the ranking of important uncertain variable depends on the version of the code used for the design. De Felice *et al.* [4] propose an effective fragility analysis method for assessment of seismic reliability of reinforced concrete bridges. Different sources of uncertainty considered were: (i) seismic input, through the use of different accelerograms for dynamic analysis, (ii) the structural behaviour, through the use of nonlinear finite element program, (iii) the variables contributing to the ultimate limit state. They have carried out reliability analysis of RC bridge piers also. Choe *et al.* [5] presented the concept of fragility increment function which when applied on the fragility of undeteriorated reinforced concrete column would give rise to the fragility of the deteriorated column at any given time. They consider the chloride induced corrosion of reinforcement in the bridge column to be the cause of degradation in the structural capacity. Though this study has not carried out seismic fragility analysis, the concepts

developed by Choe *et al.* [5] are useful. This type of analysis would be useful for life cycle cost- and risk- analyses. Benamer and Feng [6] carried out discrete element/finite element based analyses of reinforced concrete bridge piers subjected to different earthquakes (of varying intensities and durations). Though this study does deal with classical reliability analysis, important conclusions that can be useful in future reliability analyses are drawn. They are, amongst others, the rate of loading influences the damage pattern, affecting the ductility mobilized at collapse; the effect of confinement action in the plastic zone depends on the level of axial force on the pier. Frangopol and Akiyama [7] presented a methodology for carrying out seismic analysis of reinforced concrete bridges located in aggressive environment causing corrosion of reinforcement. They applied the proposed methodology to determine the seismic reliability of reinforced concrete bridge piers with corroded steel reinforcement. Based on this analysis they established a relation between the amount of steel corrosion and the seismic reliability of the pier. It has been found that the corrosion of steel reinforcement significantly reduces the reliability of bridge pier. Recently, Biondini *et al.* [8] have brought out the importance of integrating the concepts of time variant reliability analysis and nonlinear static analysis of bridge system taking into account the possible deterioration of performance of the system due to corrosion of reinforcement. From their study they concluded that the reliability of bridge pier is important in ensuring the system safety.

From the brief review of literature presented above, it is noted that there is a need to evolve a practical method for seismic reliability analysis of RC bridge piers taking into account the recent developments in defining the performance limit states. In this paper an attempt has been made to determine the reliability of reinforced concrete bridge column having a circular cross-section and subjected to North Ridge Earthquake [14]. The bridge pier system is idealized as a SDOF. However, the methodology presented in this paper is general and can be applied to even MDOF systems also. The problem presented in this paper is considered because results of tests on models of the bridge pier are available in the literature; and hence it is possible to compare the results of nonlinear dynamic analysis with the relevant experimental results. For determination of the moment-curvature and base shear-top displacement relationships of the cross-section, USC_RC program [13] which implements the plastic hinge model (as proposed by Priestly *et al.* [9]) is used. Limit states of serviceability and damage control as defined by Kowalsky [10] are considered for the reliability analysis. The organization of the paper is shown in Chart 1.

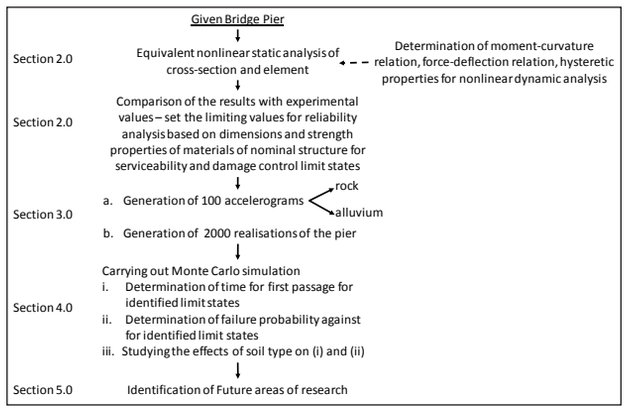

Chart 1 Organization of the paper

2. Non-Linear Analysis of Pier

The Moment-curvature analysis and Force-deflection analysis of the pier, whose dimensions are same as that of test specimen as described in Hachem *et al.* [1], are carried out using USC_RC program (USC_RC, 2006). The details of the bridge pier considered are given in Appendix. Non linear time history analysis is performed on the pier using STEPS program given by Paz [11] and the results are compared to the experimental results as reported in Hachem *et al.* [1].

2.1 Material Modeling

Reinforcing Steel

The steel reinforcement is modeled as a bilinear backbone curve as shown in Fig. 1.

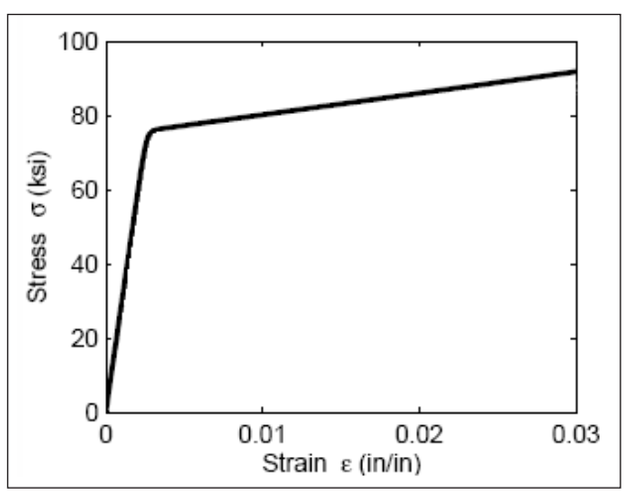

Fig. 1 Stress Strain curve for Steel model

Concrete

Concrete properties are modeled by using the Mander's stress strain model for confined and unconfined concrete. The model is parabolic up to the maximum compressive strength f1c. The relation by Mander was used to compute enhanced strength f1cc and strain capacity ε_{cu} of confined concrete can be seen below. Manders stress strain model for confined and unconfined concrete are shown in Fig. 2.

Confined compressive strength can be computed as

$$f_{cc}^{'} = f_{co}^{'}\left[-1.254 + 2.254\sqrt{1+\frac{7.94\,f_l^{'}}{f_{cc}^{'}}} - \frac{2\,f_{cc}^{'}}{f_{co}^{'}}\right] \quad (1)$$

where $f_{co}^{'}$ is unconfined concrete compressive strength, $f_1^{'}$ is the effective confining stress.

$$f_l^{'} = k_e\, f_l \quad (2)$$

Where k_e can be taken as 0.95 for circular sections and f_l is given by

$$f_l = \frac{1}{2}\rho_{sp}\, f_{yh} \quad (3)$$

where ρ_{sp} is spiral reinforcement volumetric ratio, f_{yh} is spiral reinforcement yield strength

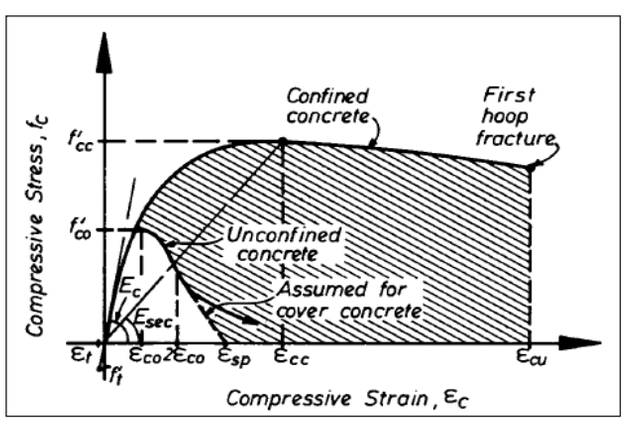

Fig 2 Mander's stress strain model for confined and unconfined concrete

2.2 Analytical Models

A number of non-linear models are available for modeling reinforced concrete member behavior. A number of different models are used in literature to simulate the column tests and are compared in terms of accuracy and complexity. The nonlinear models used can be divided into two categories namely Plastic hinge models and Finite element models. In this paper, a plastic hinge model is used to model the nonlinear force-deflection behavior of reinforced concrete column.

Plastic hinge model

The model chosen is a bilinear model with effective stiffness EI_e (see Fig. 3).

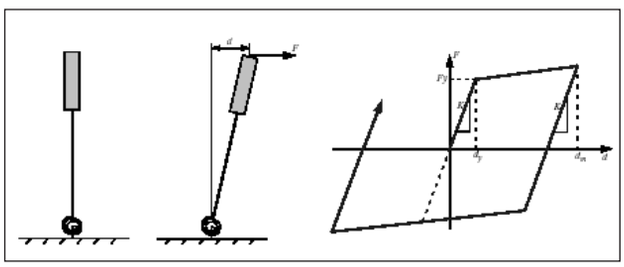

Fig 3 Bilinear model with effective stiffness EIe

Moment curvature analysis

Regardless of the numerical model used, the Engineer needs to predict the Moment curvature relation or force deflection relation. This can be used to estimate the effective sectional stiffness for an elastic model and provides the basis for computing effective properties of plastic hinges in concentrated plasticity models. In this paper, force deflection analysis for the column section, whose cross section dimensions are same as that of test specimen [1] and its material properties, as defined above, is carried out using USC_ RC program considering the column as a cantilever structure with tip mass. The screen captures of input such as sectional properties, material properties

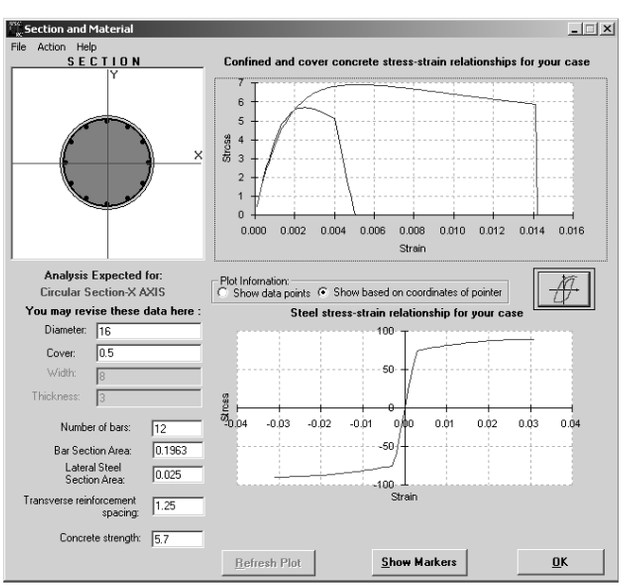

Fig 4 Section and Material properties of column in USC_RC program (FPS units)

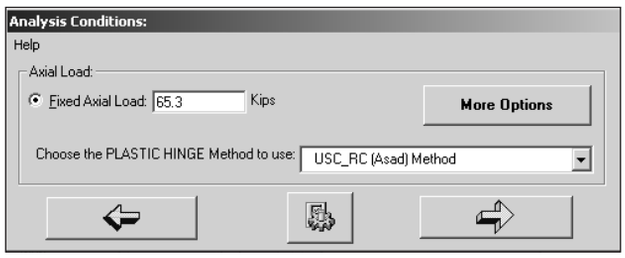

Fig 5 Axial load on column in USC_RC program

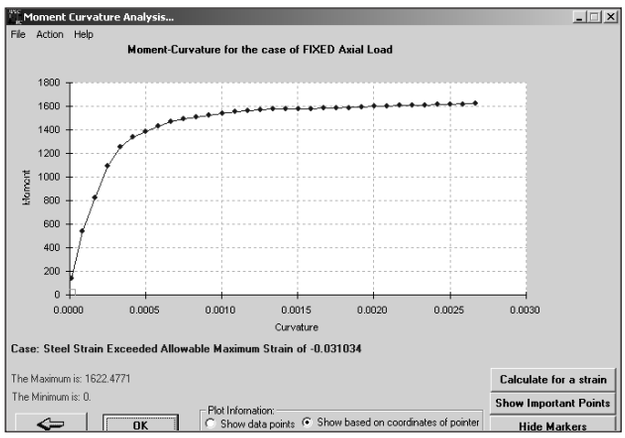

Fig 6 Moment curvature Graph of the column from USC_RC program (FPS units)

and axial load and output such as force deflection, interaction curve and moment curvature graphs are shown below. The units in the screen captures are in FPS units.

After determining the moment curvature relationship using USC_RC, the main aim is to determine the yield moment of the cross-section. This is difficult to obtain directly from Fig. 6, as it contains multiple linear segments. For this purpose, interaction surface is obtained as shown in Fig. 7 by using USC_RC and the moment corresponding to applied axial load of 65.3 kip is taken as yield moment. While the procedure given in Priestley *et al.* [9] can be followed to get M_n, in the present study, since M_y is obtained directly from interaction surface, point of interaction of lines from M_u and the line through origin and M_y can be taken as nominal moment. Using the moment curvature relation obtained, the sectional properties of the plastic hinge model of the pier are computed. The properties of cantilever column model corresponding to first yield, effective yield and ultimate are presented in Table 1. Some of the results presented in this table are compared with force-deflection analysis of the component shown in Fig. 8. From this figure it is observed that the value of ultimate shear force is 16.9 kip which occurs at an ultimate displacement of 4.55 in. The value of yield shear force as read from Fig. 8 is 11.66 kip and the corresponding yield displacement is 0.69 in. These values compare satisfactorily with those computed in Table 1. Therefore, the displacement ductility of the section is 4.55/0.79 = 5.76. The length of plastic hinge, L_p, required for estimation of displacement ductility is computed from,

$$L_p = 0.08\,L + 0.15\,f_y\,d_b \tag{4}$$

where L is the height of column from bottom to center of mass, f_y is yield stress of longitudinal steel, d_b is longitudinal bar diameter. The plastic hinge length for the present problem is estimated as 13.3 in.

Table 1 Section properties from moment-curvature analysis and plastic hinge model

Property	Yield	Effective Yield	Ultimate
Curvature ϕ (1/in)	ϕ_y = 0.00022	ϕ_{ye} = 0.000361	ϕ_u = 0.002694
Moment, M (kip-in)	M_y = 1066.7	M_n = 1533.3	M_u = 1622.4771
Shear V (kip)	$V_y = M_y/L$ = 11.11	$V_n = M_n/L$ = 15.972	$V_u = M_u/L$ = 16.9
Displacement δ (in)	$\delta_y = \phi_y (L^2/3)$ = 0.676	$\delta_{ye} = \phi_{ye} (L^2/3)$ = 1.11	$\delta_{ult} = (\phi_u - \phi_{ye}) L_p (L - L_p/2) + \delta_{ye}$ = 3.9512
Secant Stiffness k (kip/in)	V_y/δ_y = 16.435	V_n/δ_{ye} = 14.39	V_u/δ_{ult} = 4.277
Period T (sec)	0.637	0.681	1.25
Secant Stiffness EI (kip-in2)	$EI_y = M_y/\phi_y$ = 4.8X10^6	$EI_{ye} = M_n/\phi_{ye}$ = 4.246 × 10^6	$EI_u = M_u/\phi_u$ = 0.6021 × 10^6

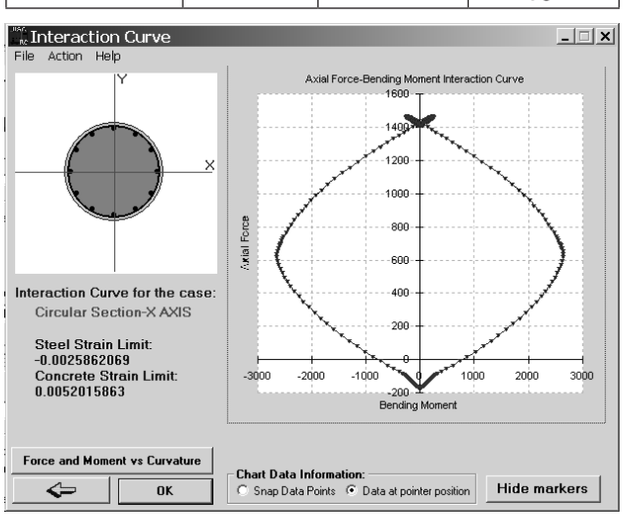

Fig 7 Interaction Curve of a column from USC_RC program (FPS units)

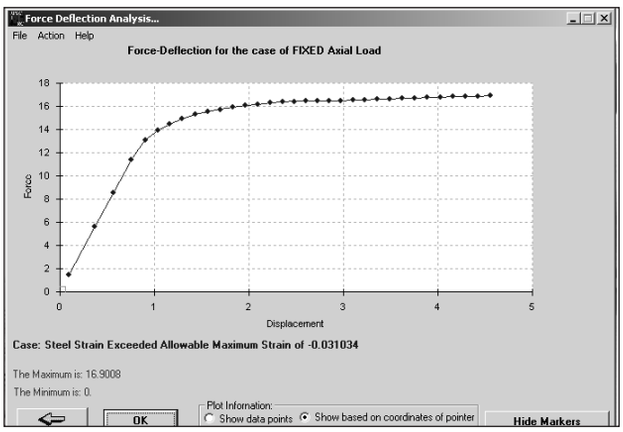

Fig 8 Force Deflection Graph of a column from USC_RC program (FPS units)

After carrying out an equivalent static analysis, a detailed non-linear time history analysis of single degree of freedom system is carried out using STEPS program [11]. The main aim of carrying out such an analysis is to compare the predicted maximum relative displacement with those observed experimentally (on the model) [1]. The seismic excitation to be provided to the structure is discussed in the following section.

2.3 Ground Motion

The chosen time history for analytical models is an approximate of the time history of the Northridge earthquake, shown in Fig. 9. The record was scaled assuming a length scale factor of 4.5, which is consistent with the scale of the specimen. Hence, the time duration of the record was reduced by 2.12, while the acceleration was kept the same. The scaled time history is shown in Fig. 10.

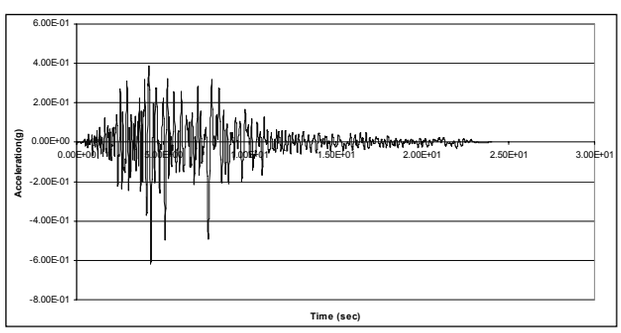

Fig 9 Actual Acceleration Time history of Northridge earthquake

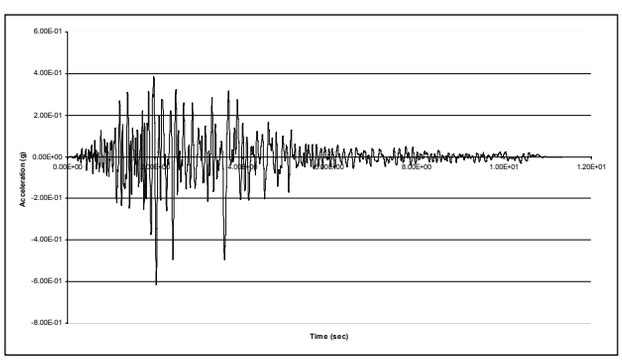

Fig 10 Input Acceleration Time history of Northridge earthquake

2.4 Non-Linear Dynamic Time History Analysis

The main aim of this paper is to develop a methodology for carrying out the reliability analysis of reinforced concrete bridge pier using nonlinear dynamic analysis of SDOF system subjected to stochastic seismic excitation. Also, an attempt is made to determine the statistical properties of the first passage time against limit states defined (see section 2.5 of this paper). The methodology is developed within the framework of Monte Carlo simulation since this is simple to use and finding its way into the design decision making in many engineering problems. In order to achieve these objectives, a deterministic nonlinear dynamic analysis program STEPS [11] is used. For STEPS program, the stiffness, restoring force, yield displacement, displacement ductility are required. These quantities are estimated using Fig. 8. The hysteretic behavior of the column is idealized by linear elastic and perfectly plastic curve. Therefore, the force-displacement relation obtained in Fig. 8 is idealized as a bilinear curve. The restoring force corresponding to yield is approximately taken as that force corresponding to effective yield and is given as 15.97 kip (Table 1). The stiffness is obtained from Fig. 8 as 15.97/1.03 = 15.52 kip/in. The mass of single degree of freedom is 0.169 kip-sec^2/in. The natural frequency of the system is 9.58 rad/sec (time period = 0.656 s).The nonlinear dynamic response of the bridge pier subjected to the seismic excitation (Fig. 10) is shown in Fig. 11. From Fig. 11, it can be noted that once the absolute value of the relative displacement exceeds effective yield displacement value of about 1.11 in. (Table 1), the system seems to have yielded since there is a residual displacement about which the system oscillates. The maximum value of the relative displacement obtained from the analysis is about 4.7 in. which is about 17% more than the ultimate displacement value of 3.95 in. obtained from the static analysis. Thus, the STEPS program can be used for the reliability analysis of the bridge pier.

To carry out the reliability analysis, the limit states have to be first defined. The limit states considered in this investigation are useful in making engineering decisions regarding the repair/retrofit. The details of the limit states are presented in the next section.

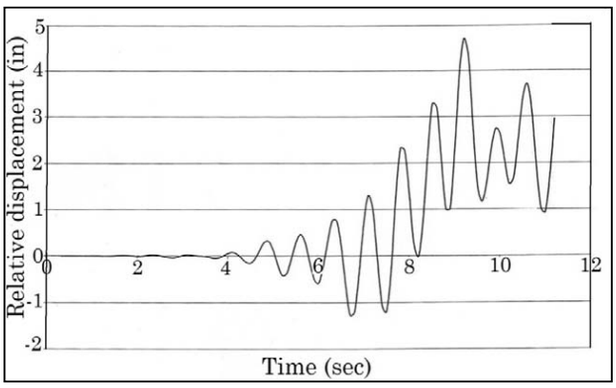

Fig. 11 Time history of relative displacement of the bridge pier considered

2.5 Definition of Limit States:

Two limit states are considered in this paper: *serviceability* and *damage control*. Qualitatively, serviceability implies that repair is not needed after the earthquake, while damage control implies that only repairable damage occurs. Quantitatively, it is assumed that these limit states can be characterized with respect to concrete compression and steel tension strain limits. These limits are presented in Table 2. The serviceability concrete compression strain is defined as the strain at which crushing is expected to begin, while the serviceability steel tension strain is defined as the strain at which residual crack widths would exceed 1 mm, thus likely requiring repair [9] and interrupting serviceability.

The damage control concrete compression strain is defined as the compression strain at which the concrete is still repairable. This assessment is subjective and is a function of the transverse reinforcement details provided. The energy balance approach developed by Mander *et al.* [12] can be utilized to estimate the ultimate concrete compression strain. Using the approach outlined by Priestley *et al.* [9] and the results of shake table tests reported by Kowalsky *et al.* [10], the compression strain in concrete corresponding to the damage control limit state is assumed as 0.018. The remaining limit state definition is related to the steel tension strain at the damage control level. The point at which repair no longer becomes feasible will likely be related to the point at which incipient buckling of reinforcement occurs, which may be related to the peak tension strain sustained in the previous loading cycle. The steel tension strain must also be limited to avoid rupture of reinforcement while allowing for the reduction in strain capacity due to cyclic loading.

It is noted that the damage control level strain limits assume well-detailed systems, and would not be appropriate for assessment of existing columns with insufficient transverse reinforcement. In the case of the serviceability limit state, the proposed strain limits are felt to be widely accepted.

Table 2 Limit state definitions [9]

Limit state	Concrete strain limit	Steel strain limit
Serviceability	0.004 (compression)	0.015 (tension)
Damage control	0.018 (compression)	0.060 (tension)

For the bridge pier considered, the moments, shears and the top displacements corresponding to the limiting values of strain presented in Table 2 are evaluated. The results obtained are presented in Tables 3 and 4. The limit state of damage control regime is controlled by the failure of steel in tension as the strain in steel achieves an allowable value of 0.03, for the steel considered in this investigation. The top displacements presented in Table 4 are considered to be allowable values in the reliability analysis. This is a reasonable assumption since the values are obtained based on dimensions, material properties, and excitation corresponding to the nominal structure.

Table 3 Moments, curvatures and base shears corresponding to the two limit states considered for the bridge pier considered (with nominal properties) obtained from USC_RC

Limit State Considered	Moment M_i (kip-in)	Curvature Φ_i (in/in)	Neutral axis depth (in)	Base Shear $V_i=M/L$ (kips)
Serviceability $\varepsilon_c = 0.004$	1554.18	0.001082	3.697	16.189
$\varepsilon_s = -0.015$	1565.50	0.001167	3.652	16.307
Damage Control $\varepsilon_c = 0.018$	533.87	0.00863	0.0855	This state is not reached since failure occurs earlier due to the exceedance of allowable strain in steel first (see Fig. 1)
$\varepsilon_s = -0.03$	1612.24	0.00234	3.669	16.794

Table 4 Base shear and corresponding top displacement of the pier obtained from USC_RC

Base Shear V_i (kips)	Tip displacement δ_i (in)
≈ 16.189	1.789
≈ 16.307	1.994
≈ 16.794	3.50

3. Reliability Analysis of the Bridge Pier

The methodology adopted in this study consists of the following steps:

1. Generate one hundred non-stationary acceleration time histories corresponding to the details presented in Table 5.
2. For each time history generated, generate an ensemble of two thousand nonlinear displacement response time histories of the system. The system random variables are those presented in Table 6. All the variables are assumed to follow lognormal distribution.
3. A sample of 0.2 million time histories of the response is thus generated. It is assumed that the pier fails in a given limit state 'i' (i = 1,2,3 as given in Table 4) if the absolute value of the displacement equals or exceeds the allowable values specified in Table 4. Also, the times at which the first passage of the violating the limit states are evaluated for each of the 0.2 million time histories.
4. The probabilities of failure are reported for different limit states using the relative frequency approach. In calculating the statistical properties of the times to failure, however, only those samples in which the limit states are violated need to be considered.
5. The steps 1-4 are repeated for two types of soils considered whose details are presented in Table 5.

Table 5 Details of deterministic envelope function used for generating the stochastic earthquakes

$A_0 = 1$; PGA = 0.61g; Duration = 11.2 sec

$$a(t) = \begin{cases} A_0\,(t/2)^2 & 0 < t < 2 \text{ sec} \\ A_0 & 2 < t < 3.89 \\ A_0\left[e^{-0.992(t-3.89)}\right] & 3.89 < t < 6.62 \\ A_0\,[0.05 \text{ x } 1 + 0.0005(11.2 - t)^2] & 6.62 < t < 11.2 \end{cases}$$

Rock: Ground Frequency (f_g) = 4.30, Ground Damping(ξ_g) = 0.34, Ground Intensity (G_0) = 0.070.

Alluvium: Ground Frequency (f_g) = 2.92, Ground Damping(ξ_g) = 0.34, Ground Intensity (G_0) = 0.102.

Smooth power spectral density of the ground acceleration has been commonly presented in the form proposed by Kanai and Tajimi as a filtered white noise ground excitation of spectral density G_o in the form

$$G(\omega) = \frac{1 + 4\xi_g^2(\omega/\omega_g)^2}{\left[1 - (\omega/\omega_g)^2\right]^2 + (2\xi_g\omega/\omega_g)^2} G_0$$

The Kanai-Tajimi parameters ξ_g, ω_g, and G_0 represent ground damping, ground frequency, and ground shaking intensity.

Table 6 System variables considered to generate response time histories

Random Variable	Mean	COV
Mass m (kip-sec^2/in)	0.169	0.05
Stiffness k (kip/in)	15.52	0.15
Restoring force F (kip/in)	15.97	0.15
Damping coefficient C (kip-sec/in)	5%	0.30

4. Results

The results obtained from the reliability analysis are presented in Figs. 12-15. As expected, the values of mean time to first passage with respect to serviceability limit states are almost the same for a given type of soil. The same trend is observed for the range of first passage times. This indicates that these two limit states are reached almost simultaneously. However, there is a marginal increase in the mean time to reach the damage control limit state. The ranges of first passage time corresponding to serviceability limit states show larger scatter for rock than for alluvium soil. This may be because, the response of the system is more sensitive to the elastic properties when the system is located on rock, and the variations in the elastic properties give rise to larger scatter in the first passage time corresponding to serviceability limit states. The range of first passage time corresponding to the damage control limit state exhibits larger scatter for alluvium soil than for the rock. This could be due to the fact that the energy content of the Kanai-Tajimi spectrum around the system natural frequency (=1.52 Hz) is more for alluvium than for the rock. Determination of statistics of the first passage times would be useful in the design of active control systems.

The failure probabilities of the bridge pier for the two types of soils considered are shown in Figs. 14

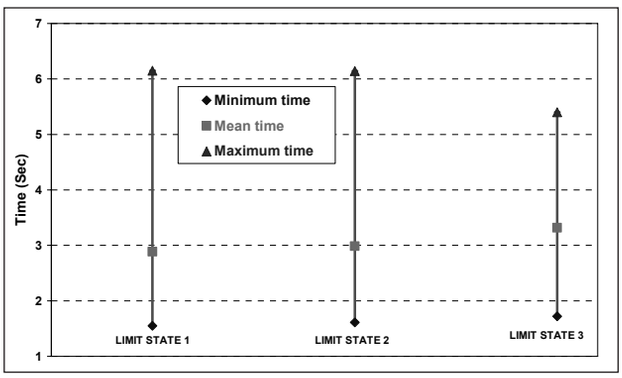

Fig. 12 Mean and range of times to first passage for the three limit states considered (soil type: rock)

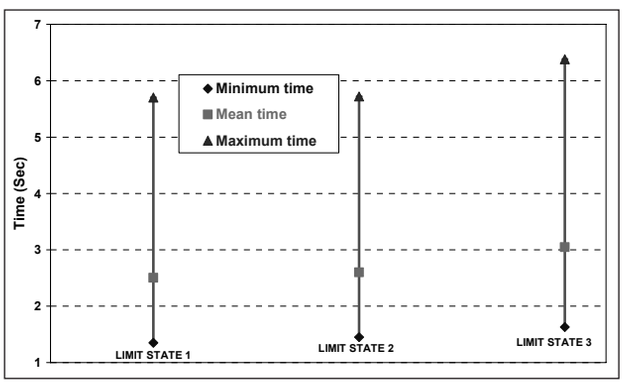

Fig. 13 Mean and range of times to first passage for the three limit states considered (soil type: alluvium)

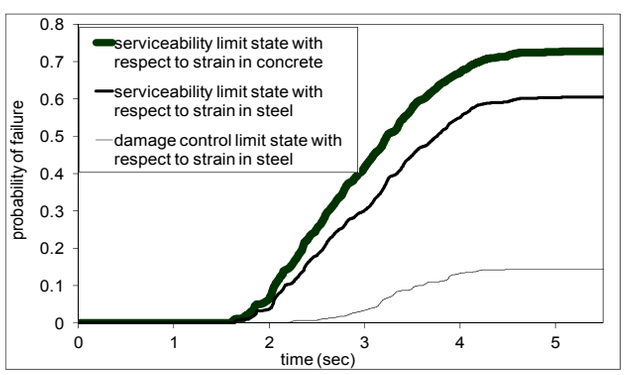

Fig. 14 Failure probability against the three limit states considered (soil type: rock)

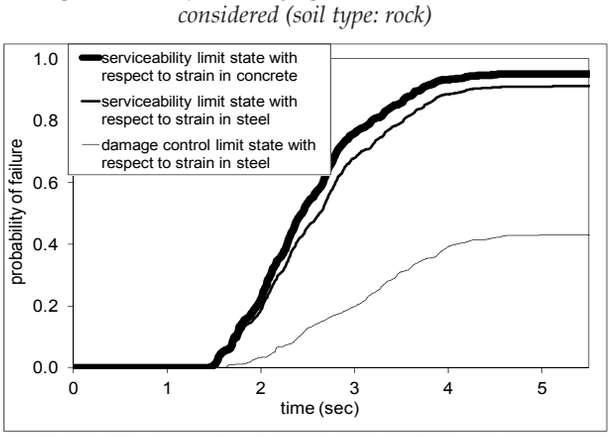

Fig. 15 Failure probability against the three limit states considered (soil type: alluvium)

and 15. While the mean and range of first passage times for the serviceability limit states 1 and 2 are almost the same for a given type of soil, it is noted from Figs. 14 and 15 that the probability of attaining serviceability limit state due to straining in concrete is more likely, irrespective of the soil type. This also suggests that, at any given time, the pier undergoing extensive damage due to spalling of cover concrete is more likely than failure through developing residual cracks in cover concrete. It is also noted from Figs. 14 and 15 that the failure probabilities against different limit states are higher for the alluvium soil. This could be attributed to higher energy content of the Kanai-Tajimi spectrum around the system natural frequency (=1.52 Hz) for alluvium than for rock. This shows the importance of using site-specific accelerograms for reliability analysis. The final failure is governed by failure of longitudinal steel, than the failure of core concrete. Thus, by carrying out a reliability analysis, it is possible to identify the likely failure regimes for the bridge pier.

5. Conclusions

A methodology for seismic reliability analysis of reinforced bridge piers against different limit states is developed. The methodology is general and practical, which can be applied for engineering decision making. In the proposed methodology, the probability of failure is determined by posing as a first passage problem in a Monte Carlo simulation framework. The example problem of reliability analysis of a model of the prototype of a reinforced concrete bridge pier, whose results are available in literature, is considered to illustrate the proposed methodology.

The future areas of research may address the problem of setting forth the serviceability and damage control limit states for existing columns taking into account the possible deterioration due to environmental effects. These effects should also be considered in determining the system properties (viz., stiffness, restoring force, ductility) for carrying out the reliability analysis.

Acknowledgements

The paper is being published with the kind permission of Director, CSIR-Structural Engineering Research Centre, CSIR Campus, Taramani, Chennai, India.

References

1. Hachem, M.M., Mahin, S.A. and Moehle, J.P., "Performance of Circular Reinforced Concrete Bridge Columns Under Bidirectional Earthquake Loading", Pacific Earthquake Engineering Research Center Report, 2003/06, 2003.
2. Köyluoglu, H.U., Nielsen, S. R.K. and Cakmak, A.S. "perturbation solutions for random linear structural systems subject to random excitation using stochastic differential equations", Proceedings of "Dynamics of Structures" : a Workshop on Dynamic Loads and Response of Structures and Soil Dynamics, September 14-15, 1994, Aalborg University, Denmark.
3. Akiyama, M., Suzuki, M., Hong, K-N., Cameron, I.D. and Wang, W.L., "Uncertainties affecting the seismic reliability of RC bridge piers", 13th World Conference on Earthquake Engineering, Vancouver, B.C., Canada, August 1-6, 2004, Paper No. 3325.
4. De Felice, G., Giannini, R. and Rasulo, A., "A probabilistic approach for seismic assessment of RC structures: application to highway bridges", 13th World Conference on Earthquake Engineering, Vancouver, B.C., Canada, August 1-6, 2004, Paper No. 2601.
5. Choe, D-E., Gardoni, P. and Rosowsky, D. "Fragility increment functions for deteriorating reinforced concrete bridge columns", Journal of Engineering Mechanics, ASCE, Vol. 136, No. 8, August 2010, pp. 969-978.
6. Benamer, M.O. and Feng, Y.T., "Seismic reliability of reinforced concrete bridge columns based on damage approaches", 3rd South-East Conference on Computational Mechanics – an ECCOMAS and IACM Special Interest Conference, Editors: M. Papadrakakis, M. Kojic and I. Turner, 12 – 14 June 2013, Greece.
7. Frangopol, D.M and Akiyama, M., "Lifetime seismic reliability analysis of corroded reinforced concrete bridge piers", in, Computational Methods in Earthquake Engineering, Editors: Papadrakakis, M., Fragiadakis, M and Lagaros, N.D. Springer Dordecht Heidelberg, 2011, pp. 527 – 538.
8. Biondini, F., Camnasio, E and Palermo, A., "Lifetime seismic performance of concrete bridges exposed to corrosion", Structure and Infrastructure Engineering, Vol. 10, No. 7, 2013, pp. 880-990.
9. Priestley, M.J.N., Seible, F. and Calvi, G.M. (1996), Seismic Design and Retrofit of Bridge Structures, Wiley, New York.
10. Kowalsky, M.J., Priestley, M.J.N. and Seible, F., Shake Table Testing of Lightweight Concrete Bridges, Struct. Sys. Res. Proj. SSRP-97/10, Dept. of Structural Engineering, University of California-SanDiego, La Jolla, California, 1997.
11. Paz, M., Structural Dynamics: Theory and Computation, Kluwer Academic Publications, 1997.
12. Mander, J.B., Priestley, M.J.N. and Park, R., Theoretical stress-strain model for confined concrete, Journal of Structural Division, ASCE, 114(8), 1988, pp. 1804-1825.
13. Esmaeily, A., USC-RC - Software for analyzing behaviour of a single reinforced concrete member, Version 1.0.2, USC Civil.
14. Balaji Rao, K., Anoop, M.B., Balasubramanian, S.R. and Lakshmanan, N., Reliability Analysis of Reinforced Concrete Bridge Piers subjected to Earthquakes", SERC Project Report No. SS-OLP11641/COR12-RR-2006-6, CSIR-Structural Engineering Research Centre, November 2006.

APPENDIX

The prototype column has a circular cross section with a diameter of 6ft (1.83m), and is fixed at the base and pinned at the top. The axial load in the prototype column was taken to be $0.1A_g f_c^{'}$ based on the nominal strength specified for the concrete (3250 psi or 22.4 MPa). Each column was designed to withstand demands estimated using the ARS response spectrum corresponding to stiff soil sites representing alluvium with depth of 10ft to 80ft, with 0.7g peak acceleration, and 5% structural damping. The diameter of the model column was taken as 16 inch, which corresponds to a prototype to model length scale factor of 4.5. The cross-sectional details of the test specimen are shown in Fig. A-1.

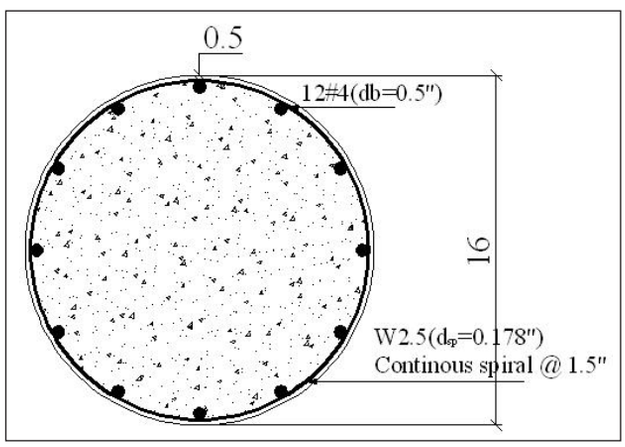

Fig. A-1. Cross section details of test specimen

The main dimensions of the specimen are given below.

D = 16 in = 406.4 mm = outside diameter of the column section

$A_g = \pi D^2/4$ = 201.64 in^2 = 129.7×10^3 mm^2 = Gross area

$I_g = \pi D^4/64$ = 3217 in^4 = 1.339×109 mm^4 = Gross second moment of inertia

C = 0.5 in = 12.7 mm = clear cover to spiral

$D_c = D - 2C - d_{sp}$ = 14.82 in = 376.4 mm = core diameter measured to the center of spiral

L = 8ft = 96 in = 2438.4 mm = Height of the column measured from the top of footing to the center of the mass consisting of the top slab and the three mass blocks.

$A_c = \pi D_c^2/4$ = 172.5 in2 = 112.3x103 mm2 = core area

P = 65.3 kips = 290.5 kN = Axial load on the column neglecting column own self weight

d_b = 0.5 in = 12.7 mm = longitudinal bar diameter (#4)

d_{sp} = 0.178 in = 4.52 mm = spiral reinforcement diameter (W2.5 plain bar)

S = 1.25 in = 31.75 mm = pitch of spiral reinforcement

Life Cycle Reliability and Safety Engineering
Vol.3 Issue 3 (2014) 42-48

Bayesian Approach on Software Reliability Modelling

D.Damodaran, R.Muthukumar
Centre for Reliability, STQC Directorate, Department of Electronics and IT (DeitY), V.S.I.Estate, Thiruvanmiyur, Chennai-600041, India
damodaran@stqc.gov.in

Abstract

Reliability Statistics has been relying on two major paradigms namely frequent and Bayesian. The frequent or classical approach believes that all distribution/model parameters are fixed values. On the other hand, Bayesians believe that these model parameters are random variables and have a distribution of their own. Bayesian statistics is becoming a considerable force to reckon with in the modeling of a random phenomenon. Hence, practitioners are increasingly turning to Bayesian methods for the analysis of complex data and complicated Reliability models. The Bayesian approach treats these population model parameters as random, not fixed quantities. Before looking at the current failure data, use is made of old information, or even subjective judgments, to construct a prior distribution model for these parameters. Bayesian Analysis have been widely used in hardware reliability assessment by constructing a joint distribution using failure time distribution and prior distribution of the parameters and finally posterior distribution is also being arrived for reliability parameters such as Mean Time Between Failures (MTBF), Failure rate etc.

Similar Bayesian approach has been applied for the Software Failure data and as a result of that several Bayesian Software Reliability Models have been formulated for the last three decades. A Bayesian approach to software reliability measurement was taken by Littlewood and Verrall (1973) and they modeled hazard rate as a random variable. One of the parameters of the distribution of this random variable is assumed to vary with the number of failures experienced. Hence it characterizes reliability change. Littlewood and Verrall (LV) proposed various functional forms for the description of this variation. These functional forms basically describe the quality debugging and an efficient programmer will have a more rapidly increasing function than an in-efficient programmer. In LV model, it is assumed that failure times follow exponential distribution and the prior distribution follows gamma distribution.

The s- shaped model proposed by Yamada et al is a potential model in the NHPP category which takes into account the learning process through which the users become familiar with the software and test tools. In Yamada's model the Erlang distribution has been embedded in its mean value function and failure intensity function. It is well known that Erlang distribution has wide applicability in several areas including telephone traffic, engineering and queuing systems. In this paper a new Bayesian Software Reliability model is presented. Times between failures follow Erlang distribution with stochastically decreasing order on the failure rate functions of successive failure time intervals with the software tester's intention to improve the software quality by the correction of each failure. With the Bayesian approach, the predictive distribution has been arrived at by combining Erlang time between failures and gamma prior distribution for the parameter of the failure rate. The expected time between failure measure, reliability function etc. have been obtained. The posterior distribution of the failure rate parameter has been deduced and the mean failure rate parameter is also obtained. For the parameter estimation, Maximum likelihood estimation (MLE) method has been adopted. The proposed model has been applied to two sets of actual software failure data. It has been observed that the predicted failure times as per the proposed model are closer to the actual failure times. Sum of square errors criteria has been used for comparing the actual time between failure times and predicted time between failures.

Keywords: Software reliability, Bayesian approach, Erlang distribution

1. Introduction

The world of statistics is traditionally divided into two mutually exclusive camps and they are Bayesian and Classical. Bayesian Statistics is the extension of conditional probability which is being calculated based on some prior information. The Classical statistician believes that all distribution parameters are fixed values. On the other hand, Bayesians believe that parameters are random variables and have a distribution of their own. Bayesian statistics is becoming a considerable force in the modelling of a random phenomenon. Hence, practitioners are increasingly using Bayesian methods for the analysis of complex data and complicated Reliability models. Before looking at the current failure data, use is made of old information, or even subjective judgments, to construct a prior distribution model for these parameters.

1.1 Hardware Bayesian Reliability Analysis

Bayesian Analysis have been widely used in hardware reliability assessment by constructing a joint distribution using failure time distribution and prior distribution of the parameters and finally posterior distribution is also being arrived for reliability parameters such as Mean Time Between Failures (MTBF), Failure rate etc. Let us assume Mean Life (MTBF) of a hardware device is ranging from 80 to 120 hours following some pattern. The life t of that Hardware device follows the Exponential distribution with parameter MTBF (Mean) θ with probability density $f(t)=\frac{1}{\theta}Exp\left(-\frac{t}{\theta}\right)$ and the parameter MTBF (θ) is random variable having a statistical distribution for example Uniform Distribution (80,120) with the following probability density function [1]

$$f(\theta)=\frac{1}{120-80}=\frac{1}{40};\ \text{for } 80<\theta<120 \tag{1}$$

Then the Joint Distribution f(t1,t2,.....tn, θ) of both the hardware failure data and the Mean parameter θ, by multiplying their Conditional and Prior distributions can be obtained by as follows:

$$\frac{1}{\theta^n}Exp\left(-\frac{\sum t_i}{\theta}\right)*\frac{1}{40}=\frac{1}{40\theta^n}Exp\left(\frac{\sum t_i}{\theta}\right);\text{for } 80<\theta<120 \tag{2}$$

Then the Marginal distribution of the sample data can be obtained by integrating the Joint Distribution, for all possible values of the parameter MTBF (θ) as follows:

$$=\int_{80}^{120}\frac{1}{40\theta^n}Exp\left(\frac{\sum t_i}{\theta}\right)d\theta \tag{3}$$

And finally, we can obtain the Posterior distribution of parameter θ (MTBF), which is the distribution of θ, combined with available hardware failure data information.

$$Posterior=\frac{Joint\ Distribution}{Marginal Distribution}$$

$$=\frac{\frac{1}{\theta^n}Exp\left(-\frac{\sum t_i}{\theta}\right)}{\int\frac{1}{\theta^n}Exp\left(-\frac{\sum t_i}{\theta}\right)d\theta} \tag{4}$$

From the above Posterior distribution, we can estimate Expected Mean life (MTBF). Similar approach can be extended to Bayesian Software Reliability Analysis.

1.2 Software Bayesian Reliability Estimation

During the last three decades, many software reliability models have been proposed, studied and modified for assessing software reliability and for estimating the reliability growth [2],[3],[4],[5] and [6]. The Software reliability models have been broadly classified into either of the categories, namely, time between failure models and fault count models. The most common approach is that time between failures follows a known probability distribution and the parameters of which depend on the number of faults remaining in software during this interval of failure times [3]. Many of the existing software reliability models have been formulated within the classical framework where software–failure times are assumed to be distributed according to a member of given parametric family of distributions whose parameters are estimated from the past failure data of the system and these parameters are thought to be unknown, but fixed quantities. Parameter estimation in the existing Markov and Non homogeneous Poisson process (NHPP) models is not an easy task and sometimes these estimates do not provide adequate results [7]. The Bayesian approach utilizes experiences from similar software assignments and previous information about the software development projects with the available failure data in order to make accurate estimation and prediction. Bayesian approach ([8] and [9]) has proven to be an effective methodology since it allows the incorporation of prior information such as expert knowledge, historical data, etc. into the model, thus improving its prediction on software reliability while reducing testing time and sample size requirements. Several Bayesian models have been proposed for the analysis of software failure data combined with

preceding knowledge in the form of so called prior distribution of the unknown parameters ([10] and [11]). The celebrated Littlewood–Verall (LV) Bayesian model is the pioneering model in this category of software reliability models. This model does not attempt analyzing in terms of the number of errors in the software programme but instead have concentrated on treating failures of the programme. The LV model has been developed on assuming that failure time distribution as exponential which is realistic and the prior distribution of the parameter is a gamma which is mathematically tractable. However, Littlewood (1979) has observed that "tentative evidence is presented that non exponential distributions of the LV model are superior to the simple exponential distributions of other models". The s-shaped model developed by Yamada et al (1984)[12] under the NHPP type of models takes into account the learning process through which the users become familiar with the software and test tools (Xie (1991)[7]). We have proposed in this paper, a software reliability model that the failure time distribution is following Erlang distribution which is embedded in the failure intensity function of s-shaped model. It is well known that Erlang distribution has wide applicability in several areas including telephone traffic, engineering and queuing systems. The developed model in this paper, predicts better than the LV model. The paper is organized as under. In section II, the notations and model assumptions are presented. We discuss about the proposed Bayesian software reliability model and methodology for estimation of parameters in section III. The proposed model has been validated using two actual software reliability datasets and the results are provided in section IV. Conclusions of the paper are presented in section V.

2. Bayesian Software Reliability Model based on Erlang distribution

2.1 Notations

T_i	random variable (r.v.) which represents the actual time between failures *(i-1)*th and *i*th software failure
t_i	realization of the r.v. T_i
λ_i	parameter of failure rate function at *i*th failure time.
$g(\lambda_i / \alpha, \psi(i))$	gamma prior distribution of the parameter λ_i
$\alpha, \psi(i)$	hyper-parameters
$\pi(\lambda_i / \alpha, \psi(i))$	Posterior distribution of the parameter λ_i

2.2 Model Assumptions

1. The time interval after repair of (i-1)th and the occurrence of ith failure is a random variable following a Erlang distribution.
2. Upon observing a failure, faults are immediately removed within negligible time.

We consider here, a Bayesian software reliability model which assumes Time between failures (TBFs) follow Erlang distribution. The pdf of Erlang is given by,

$$f(t_i / \lambda_i) = \lambda_i^2 t_i e^{-\lambda_i t_i}; \lambda_i > 0, t_i > 0 \quad (5)$$

where λi is the parameter of failure rate function at the i[th] failure and assume that $\lambda_i \le \lambda_{i-1}$ and it has stochastic nature as follows:

$$P(\lambda_{i-1} \le \lambda) \ge P(\lambda_i \le \lambda) \quad (6)$$

Let us assume the parameter λi (failure rate) follows gamma prior distribution with the following pdf:

$$g\left(\lambda_i / \alpha, \psi(i)\right) = \frac{(\psi(i))^{\alpha} \lambda_i^{\alpha-1} \exp(-\psi(i)\lambda_i)}{\Gamma\alpha}; \alpha > 0, \psi(i) > 0 \quad (7)$$

where a is shape parameter and $\psi(i)$ is the scale parameter depending on the number of detected faults. $\psi(i)$ may take different forms namely, $\beta_0+\beta_1 i$ (Linear), $\beta_0+\beta_1 i^2$ (Quadratic) and $\exp(\beta_0+\beta_1 i)$ (Exponential). For the different forms of $\psi(i)$, various software test environments may be described. Then the predictive distribution of t_i for the proposed Bayesian model (Damodaran, D., 2009 [13]) can be derived as follows:

$$f(t_i / \alpha, \psi(i)) = \int_0^{\infty} \left[\lambda_i^2 t_i e^{-\lambda_i t_i}\right] \frac{[\psi(i)]^{\alpha} \lambda_i^{\alpha-1} \exp\{-\psi(i)\lambda_i\}}{\Gamma\alpha}$$

$$= \frac{\alpha(\alpha+1) t_i \psi(i)^{\alpha}}{[t_i + \psi(i)]^{\alpha+2}} \quad (8)$$

Then the Mean Time Between Failure (MTBF) can be obtained as follows:

$$\begin{aligned} E(T_i) &= \int_0^{\infty} t_i \left[\frac{\alpha(\alpha+1)t_i\psi(i)^{\alpha}}{[t_i+\psi(i)]^{\alpha+2}} \right] dt_i \\ &= \alpha(\alpha+1)[\psi(i)]Beta(3,\alpha-1) \\ &= \frac{\alpha(\alpha+1)\psi(i)\Gamma 3\,\Gamma(\alpha-1)}{(\alpha+1)\alpha\Gamma\alpha} \\ &= \frac{\psi(i)\Gamma 3\,\Gamma(\alpha-1)}{\Gamma\alpha} \end{aligned} \quad (9)$$

$$\begin{aligned} MTBF &= \frac{\psi(i)\Gamma 3\,\Gamma(\alpha-1)}{(\alpha+1)\,\Gamma(\alpha-1)} \\ &= \frac{\psi(i)\Gamma 3}{(\alpha+1)} \\ &= \frac{2\,\psi(i)}{(\alpha+1)} \end{aligned} \quad (10)$$

The MTBF at $(i+1)^{th}$ failure instance can be obtained as follows:

$$E[T_{i+1}] = \alpha(\alpha+1)[\psi(i+1)]Beta(3,\alpha-1) \quad (11)$$

The posterior distribution of the parameter λ_i is as follows:

$$\pi(\lambda_i/\alpha,\psi(i)) = \frac{\left[\prod_{i=1}^{n} f(t_i/\lambda_i)\right] g(\lambda_i/\alpha,\psi(i))}{\int_0^{\infty}\left[\prod_{i=1}^{n} f(t_i/\lambda_i)\right] g(\lambda_i/\alpha,\psi(i))\,d\lambda_i} \quad (12)$$

The denominator in the right hand side of the above expression is free from λ_i after integrating with respect to λ_i and then the posterior distribution of λ_i is proportional to the numerator of the above equation and expressed as follows:

$$\pi(\lambda_i/\alpha,\psi(i)) \propto \left[\prod_{i=1}^{n} f(t_i/\lambda_i)\right] g(\lambda_i/\alpha,\psi(i)) \quad (13)$$

The mean of the posterior distribution of λ_i is derived as follows

$$\begin{aligned} E(\lambda_i) &= \int_0^{\infty} \lambda_i \prod_{i=1}^{n}\left(\lambda_i^2 t_i e^{-\lambda_i t_i}\right)\left(\frac{\lambda_i^{\alpha-1}\psi(i)^{\alpha} e^{-\lambda_i\psi(i)}}{\Gamma\alpha}\right) \\ &= (\alpha)^n(\alpha+1)^n(\alpha+2)^n \prod_{i=1}^{n} \frac{t_i\left[\psi(i)\right]^{\alpha}}{\left(t_i+\psi(i)\right)^{\alpha+3}} \end{aligned} \quad (14)$$

3. Parameter Estimation for the proposed model

The parameters of the proposed Bayesian Erlang model have been obtained by the Method of Maximum Likelihood Estimation by solving the following the Log Likelihood equations:

$$\text{Predictive } p.d.f. = \frac{\alpha(\alpha+1)t_i\left[\psi(i)\right]^{\alpha}}{\left[t_i+(\psi(i))\right]^{\alpha+2}} \quad (15)$$

Log-likelihood (*LL*)

$$LL = n\ln\alpha + n\ln(\alpha+1) + \sum_{i=1}^{n}\ln(t_i) + \alpha\sum_{i=1}^{n}\ln(\psi(i)) - (\alpha+2)\sum_{i=1}^{n}\left[\ln\left(t_i+(\psi(i))\right)\right] \quad (16)$$

For the various forms of $\psi(i)$ viz. Linear, Quadratic and Exponential the estimates of a, β_0, β_1 can be estimated by solving the respective sets of equations. The linear form has the following set of equations

$$\frac{\partial LL}{\partial\alpha} = n\left[\frac{2\alpha+1}{\alpha(\alpha+1)}\right] + \sum_{i=1}^{n}\ln(\beta_0+\beta_1 i) - \sum_{i=1}^{n}\ln\left(t_i+(\beta_0+\beta_1 i)\right) \quad (17)$$

$$\frac{\partial LL}{\partial\beta_0} = \alpha\sum_{i=1}^{n}\frac{1}{(\beta_0+\beta_1 i)} - (\alpha+2)\sum_{i=1}^{n}\frac{1}{\left(t_i+(\beta_0+\beta_1 i)\right)} \quad (18)$$

$$\frac{\partial LL}{\partial\beta_1} = \alpha\sum_{i=1}^{n}\frac{i}{(\beta_0+\beta_1 i)} - (\alpha+2)\sum_{i=1}^{n}\frac{i}{\left(t_i+(\beta_0+\beta_1 i)\right)} \quad (19)$$

For the quadratic form, we have

$$\frac{\partial LL}{\partial\alpha} = n\left[\frac{2\alpha+1}{\alpha(\alpha+1)}\right] + \sum_{i=1}^{n}\ln(\beta_0+\beta_1 i^2) - \sum_{i=1}^{n}\ln\left(t_i+(\beta_0+\beta_1 i^2)\right) \quad (20)$$

$$\frac{\partial LL}{\partial\beta_0} = \alpha\sum_{i=1}^{n}\frac{1}{(\beta_0+\beta_1 i^2)} - (\alpha+2)\sum_{i=1}^{n}\frac{1}{\left(t_i+(\beta_0+\beta_1 i^2)\right)} \quad (21)$$

$$\frac{\partial LL}{\partial\beta_1} = \alpha\sum_{i=1}^{n}\frac{i^2}{(\beta_0+\beta_1 i^2)} - (\alpha+2)\sum_{i=1}^{n}\frac{i^2}{\left(t_i+(\beta_0+\beta_1 i^2)\right)} \quad (22)$$

and for the exponential form, we have,

$$\frac{\partial LL}{\partial\alpha_1} = n\left[\frac{2\alpha+1}{\alpha(\alpha+1)}\right] + \sum_{i=1}^{n}(\beta_0+\beta_1 i) - \sum_{i=1}^{n}\ln\left(t_i+\exp(\beta_0+\beta_1 i)\right) \quad (23)$$

$$\frac{\partial LL}{\partial \beta_0} = \alpha n - (\alpha + 2)\sum_{i=1}^{n} \frac{\exp(\beta_0 + \beta_1 i)}{(t_i + \exp(\beta_0 + \beta_1 i))} \quad (24)$$

$$\frac{\partial LL}{\partial \beta_1} = \frac{\alpha n(n+1)}{2} - (\alpha + 2)\sum_{i=1}^{n} \frac{i\exp(\beta_0 + \beta_1 i)}{(t_i + \exp(\beta_0 + \beta_1 i))} \quad (25)$$

The estimation of the hyper-parameters a, β_0, β_1 has been carried out by using the above MLE equations and using C++, Software package (Turbo C++, 2008[14]).

4. Model validation with software reliability data sets

The proposed Bayesian model based on Erlang distribution, has been validated using two actual

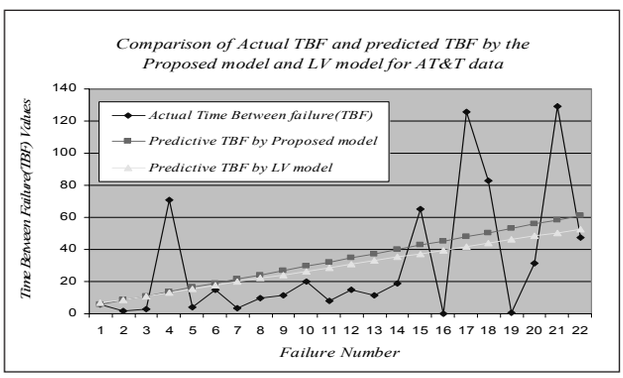

Fig. 1. Comparison of Actual TBF and predicted TBF by the proposed model and LV model for AT&T data

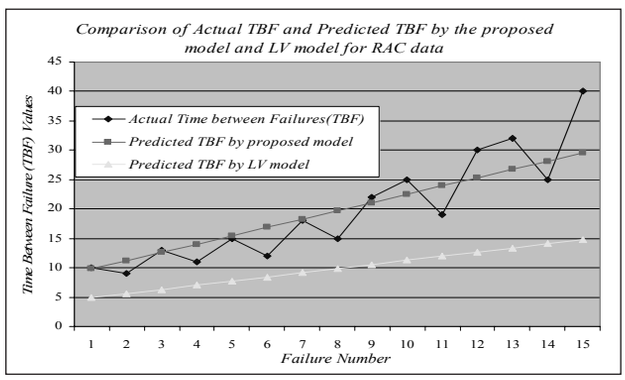

Fig. 2. Comparison of Actual TBF and predicted TBF by the proposed model and LV model for RAC data

Table 1 Comparison of predictive power of the proposed model with actual failure times in CPU units for AT&T dataset (Pham and Pham 2000)

Failure number	Actual failure times	Predictive times - new model	Predictive times - LV model	New Model - SSE	LV Model - SSE
1	5.5	5.87	6.63	0.14	1.28
2	1.83	8.50	8.827	44.51	48.96
3	2.75	11.13	11.02	70.22	68.39
4	70.89	13.76	13.22	3264	3325.8
5	3.94	16.39	15.42	154.9	131.8
6	14.98	19.01	17.61	16.28	6.92
7	3.47	21.64	19.81	330.3	267.00
8	9.96	24.27	22.01	204.8	145.20
9	11.39	26.90	24.2	240.5	164.10
10	19.88	29.53	26.4	93.09	42.51
11	7.81	32.16	28.59	592.8	431.81
12	14.59	34.78	30.79	407.8	262.44
13	11.42	37.41	32.98	675.6	464.83
14	18.94	40.04	35.18	445.3	263.74
15	65.3	42.67	37.38	512.1	779.53
16	0.04	45.30	39.57	2048	1562.6
17	125.6	47.93	41.77	6044	7039.2
18	82.69	50.55	43.97	1032	1499.2
19	0.45	53.18	46.16	2780	2089.4
20	31.61	55.81	48.36	585.7	280.56
21	129.3	58.44	50.56	5022	6201.5
22	47.6	61.07	52.75	181.4	26.52
			TSSE=	24748	25103
			MSE=	1125	1141.1

Table 2 Comparison of predictive power of the proposed model with actual failure times for RAC DATA (1996)

Failure Number	Actual failure times	Predictive failure times proposed model	Predictive failure times LV Model	SSE for proposed model	SSE for LV Model
1	10	9.78	4.892	0.05	26.09
2	9	11.20	5.598	4.83	11.57
3	13	12.61	6.305	0.15	44.82
4	11	14.02	7.011	9.14	15.91
5	15	15.44	7.718	0.19	53.02
6	12	16.85	8.424	23.52	12.78
7	18	18.26	9.131	0.07	78.65
8	15	19.68	9.838	21.87	26.64
9	22	21.09	10.54	0.83	131.2
10	25	22.50	11.25	6.24	189.0
11	19	23.92	11.96	24.17	49.59
12	30	25.33	12.66	21.82	300.5
13	32	26.74	13.37	27.64	347.0
14	25	28.16	14.07	9.96	119.3
15	40	29.57	14.78	108.8	635.8
			TSSE=	259.28	2042
			MSE=	17.29	136.1

Table 3 Reliability Characteristics for two Software Failure Datasets

Software failure Data Set & Estimated values of the hyper parameters α, β_0, β_1	Mean Time Between Failure (MTBF)		$E(\lambda_i)$ of the posterior distribution	
	At n^{th} failure time	At $(n+1)^{th}$ failure time	At n^{th} failure time	At $(n+1)^{th}$ failure time
AT&T Data: α =20.0987, β_0=30.987, β_1=25.0987	61.068	63.696	5.18E-70	1.47E-77
RAC Data: α =20.48077, β_0=81.53, β_1=13.765	39.461	40.874	2.87E-38	2.16E-45

software reliability datasets namely, RAC (1996)[15] and AT&T (Pham and Pham 2000)[9]. Actual and predicted failure times based on the proposed model for two data sets are compared. The predicted failure times based on Littlewood-Verrall (LV) model (1973) is also computed. The tables of the two data sets along with predicted failure times based on LV Model and the proposed model along with Sum of Square Error (SSE) and Mean Square Error (MSE) are presented in this section.

5. Conclusions

In this paper Bayesian approach on Software Reliability modelling has been discussed. A new Bayesian software reliability model has been proposed. With Bayesian approach, the predictive distribution has been obtained for the proposed model. In this model, software failure times based on Erlang distribution has been combined along with Gamma prior distribution for the parameter of the failure-rate function. The MTBF has been estimated for the proposed model and Posterior Distribution also has been arrived for the parameter of the Failure rate function.

The proposed model has been validated using two software failure data sets namely AT&T and RAC. Three forms viz. linear, quadratic and exponential for the scale parameter of the prior distribution have been verified for fitting the failure data. This model is fitting well for AT&T and RAC data sets. The predictive failure times based on these models are closer to the actual failure times. The predictive times ased on this model are comparatively better when comparing to LV model. The proposed Bayesian software reliability model can be used when the failure times follows Erlang distribution.

References

1. Use of Bayesian Techniques for Reliability – START Sheets, Reliability Analysis Centre (RAC), USA
2. Goel, A.L.(1985), Software Reliability modelled: Assumptions, limitations, and applicability, IEEE Trans. Software Engineering Vol.SE-11. No.12, p 1411-1423.
3. Goel, A.L., and Okumoto,K. (1979): Time dependent error detection rate model for software reliability and other performance measures, IEEE Trans. Rel. Vol.R-28, No.3, p. 206-211.
4. Lyu, M.R.(1996): Editor, Handbook of Software ReliabilityEngineering,New York, p.104-117.
5. Kapur, P.K., and Garg R.B (1999): Contributions to Hardware and Software Reliability, World Scientific, Singapore.
6. Musa, J.D., Iannino,A and Okumoto,K (1987): Software Reliability – Measurement, Prediction and Application, McGraw-Hill Book Company, Singapore.
7. Xie, M.(1991): Software Reliability Modelling, World Scientific, Singapore.
8. Martz, H.F. and Waller,R.A (1982): Bayesian Reliability Analysis John Wiley & Sons, New York.
9. Pham, L., and Pham H (2000): Software Reliability Models with Time Dependent Hazard Function Based on Bayesian Approach, IEEE Trans. Rel. Vol.30 No.1,
10. Littlewood, B., and J.L.Verall (1973): A Bayesian reliability growth model for computer Software, Applied Statistics, Vol.22, p.332-346.
11. Mazzuchi, T.A. and Soyer,R (1988): A Bayes empirical Bayes model for software reliability, IEEE Trans. Rel., Vol.37.
12. Yamada,S., Obha,M. and Osaki,S.(1983): S- Shaped reliability growth modelling for software error detection, IEEE Transactions on reliability, Vol.R-32, No.5,pp 475-478
13. Damodaran, D.(2009): Some Contributions to Software Reliability Modeling - Ph.D. Thesis, Department of Statistics, Madras University, India.
14. Turbo C++ Software Package
15. Reliability Analysis Center, USA-1-888-RAC-USER(1996): Introduction Software Reliability: A State of the Art Review.

SRESA JOURNAL SUBSCRIPTION FORM

Subscriber Information (Individual)

_____	_____	_____	_____
Title	First Name	Middle Name	Last Name

_____ _____

Street Address Line 1 Street Address line 2

_____	_____	_____	_____
City	State/Province	Postal Code	Country

_____	_____	_____
Work Phone	Home Phone	E-mail address

Subscriber Information (Institution)

Name of Institution/ Library _____

Name and Designation of Authority for Correspondence _____

Address of the Institution/Library _____

Subscription Rates

	Subscription Quantity	**Rate**	**Total**
Annual Subscription (in India)	_____	Rs. 15, 000	_____
(Abroad)	_____	$ 500	_____
	_____		_____
	_____		_____

Payment mode (please mark)

Cheque ☐ Credit Card ☐ Master Card ☐ Visa ☐ Online Banking ☐ Cash ☐ De mand Draft ☐

Credit card Number _____

Credit Card Holders Name _____

Credit Card Holde _____